



Chemical characteristics, morphology and source apportionment of PM₁₀ over National Capital Region (NCR) of India

Rubiya Banoo · Sarika Gupta · Ranu Gadi ·
Anit Dawar · Narayanasamy Vijayan ·
Tuhin Kumar Mandal · Sudhir Kumar Sharma

Received: 29 September 2023 / Accepted: 29 December 2023 / Published online: 17 January 2024
© The Author(s), under exclusive licence to Springer Nature Switzerland AG 2024

Abstract The present study frames the physico-chemical characteristics and the source apportionment of PM₁₀ over National Capital Region (NCR) of India using the receptor model's Positive Matrix Factorization (PMF) and Principal Component Analysis/Absolute Principal Component Score–Multilinear Regression (PCA/APCS-MLR). The annual average mass concentration of PM₁₀ over the urban site of Faridabad, IGDTUW-Delhi and CSIR-NPL of NCR-Delhi were observed to be 195 ± 121 , 275 ± 141 and $209 \pm 81 \mu\text{g m}^{-3}$, respectively. Carbonaceous species (organic carbon (OC), elemental carbon (EC) and water-soluble organic carbon (WSOC)), elemental

constituents (Al, Ti, Na, Mg, Cr, Mn, Fe, Cu, Zn, Br, Ba, Mo Pb) and water-soluble ionic components (F^- , Cl^- , SO_4^{2-} , NO_3^- , NH_4^+ , Na^+ , K^+ , Mg^{2+} , Ca^{2+}) of PM₁₀ were entrenches to the receptor models to comprehend the possible sources of PM₁₀. The PMF assorted sources over Faridabad were soil dust (SD 15%), industrial emission (IE 14%), vehicular emission (VE 19%), secondary aerosol (SA 23%) and sodium magnesium salt (SMS 17%). For IGDTUW-Delhi, the sources were SD (16%), VE (19%), SMS (18%), IE (11%), SA (27%) and VE+IE (9%). Emission sources like SD (24%), IE (8%), SMS (20%), VE+IE (12%), VE (15%) and SA+BB (21%) were extracted over CSIR-NPL, New Delhi, which are quite obvious towards the sites. PCA/APCS-MLR quantified the similar sources with varied percentage contribution. Additionally, catalogue the Conditional Bivariate Probability Function (CBPF) for directionality of the local source regions and morphology as spherical, flocculent and irregular were imaged using a Field Emission–Scanning Electron Microscope (FE-SEM).

Supplementary Information The online version contains supplementary material available at <https://doi.org/10.1007/s10661-023-12281-8>.

R. Banoo · N. Vijayan · T. K. Mandal · S. K. Sharma (✉)
CSIR-National Physical Laboratory, D, K S Krishnan
Road, New Delhi 110012, India
e-mail: sudhir@nplindia.org

R. Banoo · N. Vijayan · T. K. Mandal · S. K. Sharma
Academy of Scientific and Innovative Research (AcSIR),
Ghaziabad 201002, India

S. Gupta · R. Gadi
Indira Gandhi Delhi Technical University for Women,
Kashmiri Gate, New Delhi 110006, India

A. Dawar
Inter-University Accelerator Centre, Aruna Asaf Ali Marg,
New Delhi 110067, India

Keywords PM₁₀ · PMF · PCA/APCS-MLR ·
FE-SEM · NCR-Delhi

Introduction

A large number of studies have been and are being focused on characteristics and emission sources of atmospheric aerosols (Pant & Harrison, 2013; Adam

et al., 2015; Dall'Osto et al., 2013; Paterson et al., 1999; Pant et al., 2015; Friend et al., 2013; Lang et al., 2015; Guttikonda et al., 2014; Begam et al., 2017; Sharma & Mandal, 2023; Gargava et al., 2014). Still, it is a task for scientists and environmentalists to precisely quantify the sources responsible for the poor air quality or pollution in the urban regions (Pant & Harrison, 2012). Delhi, the capital city of India, i.e. the hot spot for economy, air quality is at higher risk (Gargava et al., 2014). ~3000 metric tons of pollutant emission is recorded every day with the contribution mainly from the industrial sector, traffic sector and agriculture sector (Rizwan et al., 2013). Enhancement in these sectors ultimately boosts the scale of atmospheric pollutants like PM_{10} , $PM_{2.5}$, PM_1 , SO_x , NO_x , NH_3 and O_3 in the atmosphere. Further long-time exposure to such factors leads to diseases like cardiovascular, respiratory, neurological impairments, risk of preterm birth, mortality and morbidity (Rai et al., 2016; Gupta & Elumala, 2017; Shubhankar & Ambade, 2016). The anthropogenic and natural events are accountable for the emissions of pollutants in the atmosphere (Fuzzi et al., 2015). To grasp the consequences of atmospheric pollutants on climate and human health, adherent attention has been believed towards the chemical composition, morphology, aerosol transport and thus the source apportionment (Zeb et al., 2018).

According to the 2018–2019 report released by the Central Pollution Control Board (CPCB), the number of monitoring station over the country is 731 and the concentration of the criterion pollutants is approximately four times the threshold set by National Ambient Air Quality Standards (NAAQS) (CPCB 2018–2019). Thus, to integrate the high concentrations of criterion pollutants, receptor modelling (multivariate statistical techniques) has been accepted for the identification and quantification of atmospheric pollutant (PM_{10} , $PM_{2.5}$, PM_1) sources in a precise way at the sampling site (Hopke et al., 2006; Pant & Harrison, 2012). Receptor model, i.e. chemical mass balance (CMB), potential component analysis (PCA), edge analysis (UNMIX) and positive matrix factorization (PMF) (Banerjee et al., 2015; Belis et al., 2012; Song et al., 2006), relates the source and the receptor (Chow & Watson et al., 2002; Garcia et al., 2006; Olson & Norris, 2008; Gildemeister et al., 2017). This receptor model works on the basic foundation of mass conservation as:

$$X = G \times F + e \quad (1)$$

As X denotes the input concentration matrix of defined dimension, G is the source contribution matrix and F is the source profile matrix and e the residual matrix (Paatero & Tapper, 1994a, 1994b). Moreover, for the development of a model, the physical constraints to the system must be accepted (Hopke, 2016; Henry & Kim, 1990), i.e. final data must be imitated by the model explaining the observations, expected source composition and contribution must be non-negative as negative mass emission is not acceptable (Hopke, 2016). Previously most of the source apportionment studies in India had espoused the PCA tool (Banerjee et al., 2015), recent studies have notorious the efficiency of the PMF performance, as it incorporates with the mass concentration and the uncertainties. The basic norms for a true solution in the PMF tool embrace the ratio $Q_{true}/Q_{robust} (<1.5)$; weighted residuals for the species should have a centred normal distribution (e.g. between ± 3), right appraisal of the signal to noise sensitivity for each species for 100 successive iterations from the bootstrap (BS) test and the correlation $r^2 > 0.6$, consequently perceiving the rotational ambiguity from the displacement test (DISP). Studies as Feng et al. (2022) and Soleimani et al. (2022) explored PMF model to $PM_{2.5}$ organic tracer as polycyclic aromatic hydrocarbon in Shanghai and Isfahan city in Iran. Similarly, Lima et al. (2022) quantified the heavy metal sources in the urban street dust in Brazil using PMF approach.

Scrutinising the model with the meteorological data (wind speed or wind direction) results in a reliable outcome. Conditional Probability Function (CPF) assesses the probability of wind direction coalesced with specific threshold criteria pollutant (75th–90th percentiles) (Masiol et al., 2019). Moreover, the wind speed is allied with the wind direction and the mass concentration for the precise examination of the sources regions, i.e. Conditional Bivariate Probability Function (CBPF). The application of the CBPF study to the atmospheric pollutants is very limited in India (Bapna et al., 2013, Rai et al., 2016).

This work aims the identification and quantification of emission sources and their percentage contribution to the particulate matter (PM_{10}) over National Capital Region of Delhi, India, using the statistical multivariate tools (PCA/APCS-MLR and PMF). Morphological study has also been incorporated to explore the possible emission sources of the PM_{10}

over the NCR-Delhi. Moreover, the programmed CBPF identify the local source regions contributing to the study sites. In the previous years, a very limited study has been performed following the morphology and CBPF over NCR-Delhi.

Methodology

Site description

Increase in the urbanization and industrialization NCR-Delhi in the centre is walled with the Himalayas in the North, Indo-Gangetic plain (IGP) in the east, hot plains in the south and the Thar desert in the west, such geography adds in deteriorating the

atmosphere over NCR-Delhi. The periodical sampling (i.e. twice a week at CSIR-NPL, and IGDTUW-Delhi except Faridabad) of coarse particulate matter (PM₁₀) was performed at the terrace of the urban sites of Faridabad (28°38'N, 77°29'E), Haryana; Indira Gandhi Technological University for Women (IGDTUW-Delhi), Kashmiri-Gate (28°66'N, 77°23'E), Delhi; and CSIR-National Physical Laboratory (CSIR-NPL), Delhi (28°38'N,77°10'E) for the year 2015. Figure 1 imitates the layout for these three urban sampling sites. Moreover, these locations are walled with traffic junctions, small-large scale industries, constructions, forest, residential area etc. Our previous study (Banoo et al., 2020; Sharma et al., 2014) explored the sites and their meteorology in brief.

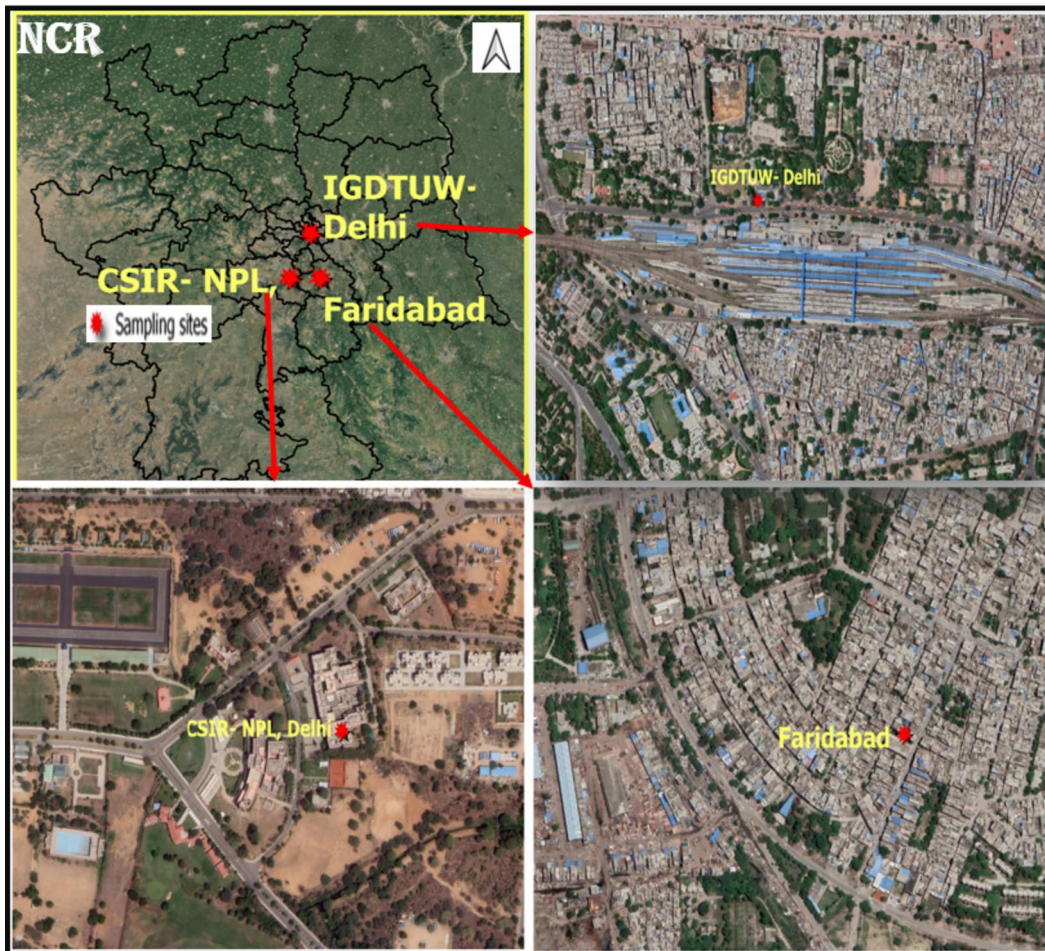


Fig. 1 Map for study sites over NCR

Sample collection

Before sampling the Pallflex quartz micro-fibres (QM-A) filters of an area ($20 \times 25 \text{ cm}^2$) were pre-baked in a furnace at a temperature of $550 \text{ }^\circ\text{C}$ for 5 h to exterminate the organic scums. These pre-baked filters were desiccated for 24 h in a controlled atmosphere. Desiccated filters were initially weighed using M/s. Sartorius microbalance (resolution $\pm 10 \text{ }\mu\text{g}$). Furthermore, initially weighed filters were carried out for 24-h sampling of PM_{10} (following the protocol defined by CPCB, Delhi, India) where the assembly of high-volume respirable dust samplers: AAS 212 NL (make: M/s. Ecotech, India; flow rate $1.2 \text{ m}^3/\text{min}$; accuracy $\pm 2\%$) was mounted on the terrace at a height of 10-m above ground level (AGL). The flow metre was calibrated with an airflow calibrator traceable to National Standard. Sampled filters were weighed and thus the gravimetric method was accepted to calculate the mass concentration as:

$$\text{Mass concentration}(\mu\text{gm}^{-3}) = \frac{(F - I) \times 10^6}{V} \quad (2)$$

Where F is the final weigh, I is the initial weight and V is the volume of the sampler defined as [$V = \text{flow rate} \times \text{sampling time}$].

Chemical analysis

Interaction of focused electron beam with the sample surface atoms can backscatter from the elastic collision reflects the information about the surface morphology. The sample is scanned by the focussed electron beam in a raster pattern (Biswas et al, 2021). The sample was prepared by cutting $5 \text{ mm} \times 10 \text{ mm}$ area of quartz filter further made adhere to the field emission scanning electron microscope (FE-SEM). This assembly was coated with platinum and positioned under vacuum condition in a spray tank so for good conductivity and reduction of electron charge. After the coating, the sample was placed into the ultra-high resolution Schottky field emission scanning electron microscope (Model: JSM-7610F) accelerating at 5 kV in a high vacuum mode. Thus, the morphology as spherical, irregular, flocculent etc. was imaged at different resolutions. Sample ID with Blank-01, FBD-23, IT-01 and NPL-05 was carried out for morphological study.

For major and trace elements (Al, Ti, Na, Mg, Cr, Mn, Fe, Cu, Zn, Br, Ba, Mo, Pb etc.) a punch of 3.0 cm diameter of the quartz filter was prepared for analysing. Such samples were positioned in WD-XRF (ZSX Primus, Rigaku, Tokyo, Japan), a non-destructive method. The detailed sample analysis procedure, principle/methodology and calibration standards used are discussed in our previous publication (Jain et al., 2017). Mathematical approach for elemental concentration is defined as:

$$\text{Elemental concentration}(\mu\text{gm}^{-3}) = \frac{(I \times E_a)}{V} \quad (3)$$

where I is the instrumentation reading, E_a is the total filter exposed area and V is the volume of the sampler.

Total organic carbon (TOC) was estimated using the assembly TOC-LCPH/CPN (M/s. Shimadzu, Japan). An area of 4 cm^2 of each filters was carried out for TOC analysis (Banoo et al., 2020). TOC is calculated as:

$$\text{TOC}(\mu\text{gm}^{-3}) = \frac{(I \times (V_x) \times (P_a \times T_a))}{V \times 10^3} \quad (4)$$

where I is the instrumentation reading, V_x is the extraction volume, P_a is the punched area, T_a is the total area and V is the volume. Thus,

$$\text{WSOC}(\mu\text{gm}^{-3}) = \text{TOC} - \text{OC} \quad (5)$$

A punch of $\sim 0.56 \text{ cm}^2$ of each filter was carried out for the analysis of organic and elemental carbon using the OC/EC analyser (Model: DRI 2001A, Atmoslytic Inc, Calabasas, CA, USA) by US EPA "IMPROVE-A Protocol" (Chow et al., 2004; Sharma et al., 2014; Jain et al., 2017). Where the concentration was estimated as:

$$\text{EC\&OC}(\mu\text{gm}^{-3}) = \frac{(I) \times (E_a)}{V} \quad (6)$$

I is the instrumentation reading, E_a is the total exposed area of the filter and V is the volume of the sampling.

Ion chromatograph with model: DIONEX-ICS-3000, CA, USA was used to estimate the amount of water-soluble inorganic species (NO_3^- , SO_4^{2-} , Na^+ , Mg^{2+} , Cl^- , F^- , K^+). The analytical error (repeatability) was estimated to be 3–7% based on triplicate ($n=3$) analysis. Previous publications (Sharma et al., 2014 a; b; Banoo et al., 2020) discussed the brief

calibration and the quality assurance/quality check (QA/QC) for the cited instrumentations. The sample blank filters were also analysed for all species and corrections were applied to maintain the QA/QC of the analysis. The method detection limit (MDL) of each chemical species (OC, EC, WSIC and major and trace elements) is calculated as three times of the average standard deviation of 10 replicates of filter blank analysis (Jain et al., 2017).

Enrichment factor (EF)

In order to identify the natural and anthropogenic sources of elements present in the aerosol samples, enrichment factors (EFs) were computed. Enrichment factor specifies the sources corresponding to the metals presented in the aerosol. Sources like crustal, anthropogenic, natural and sea salt generation are attributed to the metals in the aerosols (Taylor & McLennan, 1995; Gaonkar et al., 2020). EF of elements have been calculated using following equation (Taylor & McLennan, 1995):

$$EF = \frac{\left(\frac{E_{\text{sample}}}{X_{\text{sample}}}\right)}{\left(\frac{E_{\text{crust}}}{X_{\text{crust}}}\right)} \tag{7}$$

where elemental concentration (E_{sample}), reference element concentration (X_{sample}), elemental concentration in the upper continental crust (E_{crust}) and reference element concentration in the upper continental crust (X_{crust}) are defined accordingly. As (Al, Si, Ti and Fe) are not affected by contamination and are abundant in Earth crust, thus preferred as reference crustal elements (Saad et al., 2018). Al is considered as the reference crustal element in the present study.

Coefficients of divergence (COD)

In order to appreciate the intra-urban mass concentration variability, Wilson et al. (2005) proposed COD approach. It is defined as:

$$COD_{ij} = \sqrt{\frac{1}{n} \sum_{k=1}^n \left(\frac{X_{ki} - X_{kj}}{X_{ki} + X_{kj}}\right)^2} \tag{8}$$

where X_{ki} and X_{kj} are the k th mass concentration at i and j location, and n represents the number of data

points (Krudysz et al., 2009; Pakbin et al., 2010). COD value in the range (0–1) depicts the homogeneity in the sites, i.e. similar pattern of mass concentration. $COD > 1$ or 1 reflects the inhomogeneity in the sites thus different profiles of mass concentration (Pakbin et al., 2010). Present study showed homogeneity across the sites as Faridabad-IGDTUW-Delhi ($COD=0.039$), IGDTUW-Delhi-CSIR-NPL ($COD=0.031$) and among CSIR-NPL-Faridabad ($COD=0.026$). It was noted that among these sites, $COD \approx 0$ which means the homogeneity between the sites, thus the similarity in PM_{10} mass concentration. Kong et al. (2010) and Liu et al. (2017) reported the similarity and the dissimilarities in the concentration of polycyclic aromatic hydrocarbons (PAHs) among five cities of Liaoning province and Shanghai, China. The detailed homogeneity and inhomogeneity in the concentration of $PM_{2.5}$ and PM_{10} among the 10 sites across Los Angeles were also discussed by Pakbin et al. (2010).

Source apportionment

Positive matrix factorization (PMF)

To accomplish the PM_{10} source apportionment, present study used the US Environmental protection agency-positive matrix factorization (US-EPA PMF 5.0) software. Like other receptor models, PMF aims to work on chemical mass balance formulation (Paatero, 1997, Paatero & Tapper, 1994a, 1994b) as given in Eq. 1.

Where the weight is envisioned by minimising the function Q (global or local) and the optimal solution as:

$$Q = \sum \left(\frac{e}{U}\right) \tag{9}$$

U is the uncertainty matrix of data point, calculated as:

$$U = \begin{cases} \sqrt{(C \times E_f)^2 + (0.5 \times MDL)^2} \\ \frac{5}{6} \times MDL \text{ if } C < MDL \end{cases} \tag{10}$$

As C is the concentration, E_f is the error fraction and MDL is method detection limit (Gianini et al., 2012; Polissar et al., 1998). EPA-PMF 5.0 version

encompasses the signal/noise ratio (S/N) for each species and thus the error estimation EE (Brown et al., 2015).

$$\frac{S}{N} = \begin{cases} < 0.5 \text{Badspecies} \\ 0.5 < 1 \text{weakspecies} \\ > 1 \text{strongspecies} \end{cases} \quad (11)$$

The EE, bootstrap (BS) confront the random errors, displacement (DISP) tackles the rotational ambiguity and BS-DISP comprises the rotational ambiguity and random errors effects, thus to precisely comprehend the uncertainties (Brown et al., 2015, Norris et al., 2014).

Principal component analysis–multilinear regression (PCA-MLR)

In this study, PCA-MLR was applied to the species of PM₁₀ using the software IBM SPSS to estimate the percentile contribution of individual sources. The key objective of PCA is to reduce the dimensionality thus get the total variability of the data in a lesser number of factors with maximum variance (Larsen & Baker, 2003; Jolliffe & Cadima, 2016; Paul et al., 2013). Furthermore, to identify the percentile contribution absolute principal component score (APCS), i.e. X_k is coupled with MLR analysis (Larsen & Baker, 2003; Thurston & Spengler, 1985; Prakash et al., 2018).

Where,

$$y(\text{PM}_{10}) = \sum_{k=1}^n a_k \times X_k + b \quad (12)$$

is the multi-linear equation with a_k as slope and b as intercept, and X_k is the APCS.

The variables are normally standardized as:

$$S = \frac{\text{variablevalue} - \text{mean}}{\text{standarddeviation}} \quad (13)$$

So that, the intercept b=0, and thus variables are equated through the regression coefficients as:

$$A = \sum_{k=1}^n B_k \times X_k \quad (14)$$

To predict the modelled mass concentration and source contribution, the APCS is multiplied with the regression coefficient and thus obtained the source’s

contribution. PCA regenerated matrix error is minimized through APCS (Ogundele et al., 2016).

Conditional bivariate probability function (CBPF)

Conditional probability distribution programme was firm to scrutinize the influences of sources in various local directions. Furthermore, it gages the probability of a source positioned within a specific wind direction sector, demarcated as:

$$Y = \bar{Y} \cdot \sin\left(\frac{2\pi}{\theta}\right); X = \bar{Y} \cdot \cos\left(\frac{2\pi}{\theta}\right) \quad (15)$$

Y and X are the wind components, with θ and \bar{Y} as the average wind direction and speed. In CBPF, the individual grid mean mass concentration is calculated and differentiated (coloured) within the reference of wind speed coupled with conditional probability function (CPF) therefore discriminates the emissions source region (Uria-Tellaetxe & Carslaw, 2014).

Mathematically defined as:

$$\text{CBPF} = \frac{m_{\Delta\theta, \Delta u}}{n_{\Delta\theta, \Delta u}} \quad (16)$$

m_{Δθ, Δu} is the number of events in the wind sector and interval (Δθ, Δu) with concentration C.

n_{Δθ, Δu} is the total number of events in (Δθ, Δu).

Open air package in R-studio software is used to program CBPF (<http://www.rstudio.com/>).

Results and discussions

PM₁₀ concentration

Table 1 summarizes the annual mass concentration and chemical constituents, i.e. carbonaceous, major-trace elements and the water-soluble ionic components (WSIC) of PM₁₀ over NCR-Delhi (Faridabad, IGDTUW-Delhi, CSIR-NPL). It is studied that for all the three-study locations, the annual mass concentration of PM₁₀ is~ 3–4 times higher than the standard defined by National Ambient Air Quality Standard (NAAQS), i.e. annual—60 μg m⁻³ (Faridabad, 195 ± 121 μg m⁻³; IGDTUW-Delhi, 275 ± 141 μg m⁻³; CSIR-NPL, 209 ± 81 μg m⁻³). Enumerated the comparable mass concentration pattern by the several researchers (Gupta et al., 2018;

Table 1 Annual average concentration of the PM₁₀ constituents at the study sites of NCR

Locations Species (µg m ⁻³)	Faridabad (n=33)		IGDTUW-Delhi (n=66)		CSIR-NPL Annual (n=116) Range	
	Annual	Range	Annual	Range	Annual (n=116)	Range
PM ₁₀	195±121	44–570	275±141	58–584	209±81	69–476
EC	5.2±4.0	1.7–15.7	9.4±5.2	0.8–24.0	7.9±5.6	2–28
OC	23.6±14.4	1.7–69.1	30.8±19.3	7.8–79.4	26.0±12.8	2–72
WSOC	15.5±7.7	3.0–33.6	21.3±14.3	3.7–63.1	9.7±5.9	2.6–33
F ⁻	1.9±3.1	0.2–19.0	0.4±0.1	0.3–0.6	0.69±0.67	0.0–3.12
Cl ⁻	7.2±5.7	1.8–22.5	12.7±9.1	1.1–39.0	14.2±14.5	0.6–56.8
SO ₄ ²⁻	13.3±10.5	3.8–44.9	21.2±11.0	4.3–39.8	20.2±16.6	1.2–104.9
NO ₃ ⁻	19.3±13.0	2.5–44.7	17.0±10.7	0.0–37.9	18.9±21.8	0.0–74.5
NH ₄ ⁺	8.1±5.8	1.1–25.6	18.1±9.6	2.1–35.4	10.8±9.9	0.1–49.7
Na ⁺	3.2±4.3	0.0–25.5	2.4±0.9	0.8–5.0	2.1±1.7	0.1–14.5
K ⁺	3.1±2.0	0.0–7.8	3.7±1.8	0.7–6.2	3.9±3.7	0.4–23.4
Mg ²⁺	0.7±0.7	0.0–3.1	0.5±0.2	0.2–1.0	0.7±0.6	0.0–2.7
Ca ²⁺	3.7±3.4	0.0–14.7	3.3±1.3	1.6–5.8	9.3±6.5	0.6–33.8
Na	1.3±1.2	0.1–5.9	1.6±1.5	0.0–5.4	1.0±0.5	0.0–2.4
Al	6.9±3.6	2.2–19.5	4.7±2.4	0.7–12.6	7.1±4.5	0.8–29.8
Mg	1.4±1.3	0.3–5.4	1.2±0.6	0.1–3.3	1.7±1.1	0.3–7.4
S	4.5±2.8	0.3–10.1	4.5±3.1	1.5–13.2	5.0±2.1	2.1–12.3
Cl	4.3±4.1	0.2–15.8	2.5±2.7	0.0–17.1	6.0±4.2	0.5–19.5
K	4.3±4.8	0.5–21.2	3.7±2.1	0.6–12.1	4.1±2.2	0.0–10.9
Ca	7.4±5.8	0.9–26.9	8.8±4.1	1.0–21.1	7.4±3.7	1.6–19.5
Ti	0.5±0.3	0.1–1.2	0.3±0.2	0.0–1.0	0.4±0.3	0.0–1.7
Cr	0.1±0.0	0.1–0.2	0.3±0.1	0.1–0.6	0.2±0.1	0.1–0.3
Mn	0.1±0.1	0.0–0.4	0.1±0.1	0.0–0.3	0.2±0.4	0.0–3.5
Fe	4.4±2.9	1.5–13.3	4.2±1.8	1.0–9.8	3.3±3.3	0.1–17.8
Cu	0.2±0.1	0.0–0.6	0.2±0.3	0.0–1.5	1.8±2.4	0.0–7.2
Zn	0.6±0.5	0.1–2.3	0.8±0.7	0.1–3.0	0.4±0.2	0.0–2.1
Pb	0.2±0.1	0.0–0.6	0.5±0.7	0.0–3.8	0.4±0.3	0.0–1.6
Br	0.0±0.0	0.0–0.1	0.1±0.2	0.0–0.7	0.2±0.4	0.0–1.7

Jain et al., 2017; Mandal et al., 2014; Perrino et al., 2011; Tiwari et al., 2013) as 161±80 µg m⁻³; 285±26 µg m⁻³; 369±220 µg m⁻³; 238±106 µg m⁻³ and 183.0 µg m⁻³, respectively over Delhi. Bawase et al. (2021) recorded PM₁₀ concentration as 260±107 µg m⁻³ over Delhi-NCR. The high vehicular traffic, intricate pollution source, biomass burning, secondary aerosols, soil dust, manufacturing actions, meteorological conditions etc. might be the prime actions for such higher mass concentration (Sharma et al., 2018, Jain et al., 2020). A brief discussion of the seasonal and annual mass concentration with the carbonaceous constituents (OC, EC, WSOC, POC, SOC) has been already discussed in our previous publication (Banoo et al., 2020).

Water soluble ionic components (WSIC)

Table 1 represents the analysed nine WSIC (F⁻, Cl⁻, SO₄²⁻, NO₃⁻, NH₄⁺, Na⁺, K⁺, Mg²⁺, Ca²⁺) of PM₁₀. The pattern for WSIC was observed as for Faridabad, NO₃⁻ (19.±13.0 µg m⁻³)>S O₄²⁻ (13.3±10.5 µg m⁻³)>NH₄⁺ (8.1±5.8 µg m⁻³)>Cl⁻ (7.2±5.7 µg m⁻³)>Na⁺ (3.2±4.3 µg m⁻³). For IGDTUW-Delhi, SO₄²⁻ (21.2±11.0 µg m⁻³)>NH₄⁺ (18.1±9.6 µg m⁻³)>NO₃⁻ (17.0±10.7 µg m⁻³)>Cl⁻ (12.7±9.1 µg m⁻³)>K⁺ (3.7±1.8 µg m⁻³). For CSIR-NPL, SO₄²⁻ (20.2±16.6 µg m⁻³)>NO₃⁻ (18.9±21.8 µg m⁻³)>NH₄⁺ (10.8±9.9 µg m⁻³)>Ca²⁺ (9.3±6.5 µg m⁻³). Bawase et al. (2021) reported an analogous study of secondary inorganic ionic

species as SO_4^{2-} ($11.97 \pm 6.19 \mu\text{g m}^{-3}$), NH_4^+ ($9.95 \pm 7.16 \mu\text{g m}^{-3}$) and NO_3^- ($9.13 \pm 8.30 \mu\text{g m}^{-3}$) over Delhi-NCR. WSIC contributed (32.5%, 28% and 38%) to PM_{10} mass for the site (Faridabad, IGDTUW-Delhi and CSIR-NPL), thus dominated the major-trace elements. Sufficient quantity of ammonia is the base in atmosphere to significantly neutralize the particle fraction of nitrate, sulphate and chloride which could be achieved with the aerosol electro-neutrality relationship between ammonium (Sharma et al., 2015). Figure 2 represents a linear correlation of $2^*[\text{SO}_4^{2-}]$, $[\text{NO}_3^-]$, $2^*[\text{SO}_4^{2-}] + [\text{NO}_3^-]$ and $2^*[\text{SO}_4^{2-}] + [\text{NO}_3^-] + [\text{Cl}^-]$ concentration with NH_4^+ concentration for all the three sites. A very significant correlations was observed as $[\text{NH}_4^+]$ vs $2^*[\text{SO}_4^{2-}]$ ($R^2=0.51$; Faridabad), ($R^2=0.68$; IGDTUW-Delhi), ($R^2=0.62$; CSIR-NPL). For $[\text{NH}_4^+]$ vs $[\text{NO}_3^-]$ ($R^2=0.70$; Faridabad), ($R^2=0.87$;

IGDTUW-Delhi), ($R^2=0.68$; CSIR-NPL). For $[\text{NH}_4^+]$ vs $2^*[\text{SO}_4^{2-}] + [\text{NO}_3^-]$ ($R^2=0.84$; Faridabad), ($R^2=0.82$; IGDTUW-Delhi), ($R^2=0.69$; CSIR-NPL). $[\text{NH}_4^+]$ vs $2^*[\text{SO}_4^{2-}] + [\text{NO}_3^-] + [\text{Cl}^-]$ ($R^2=0.83$; Faridabad), ($R^2=0.80$; IGDTUW-Delhi), ($R^2=0.80$; CSIR-NPL). This significantly positive regression reflects the associations of SO_4^{2-} , NO_3^- and Cl^- with NH_4^+ . Jain et al. (2020) reported 21.2% of the secondary aerosol's contribution to PM_{10} whereas Sharma et al., (2016) reported 40% of WSIC contribution.

Major-trace elements

A total of 15 elemental species (Na, Al, Mg, S, Cl, K, Ca, Ti, Cr, Mn, Fe, Cu, Zn, Pb and Br) species were diagnosed for the locations Faridabad, IGDTUW-Delhi and CSIR-NPL of Delhi-NCR. Statistical values are comprised in

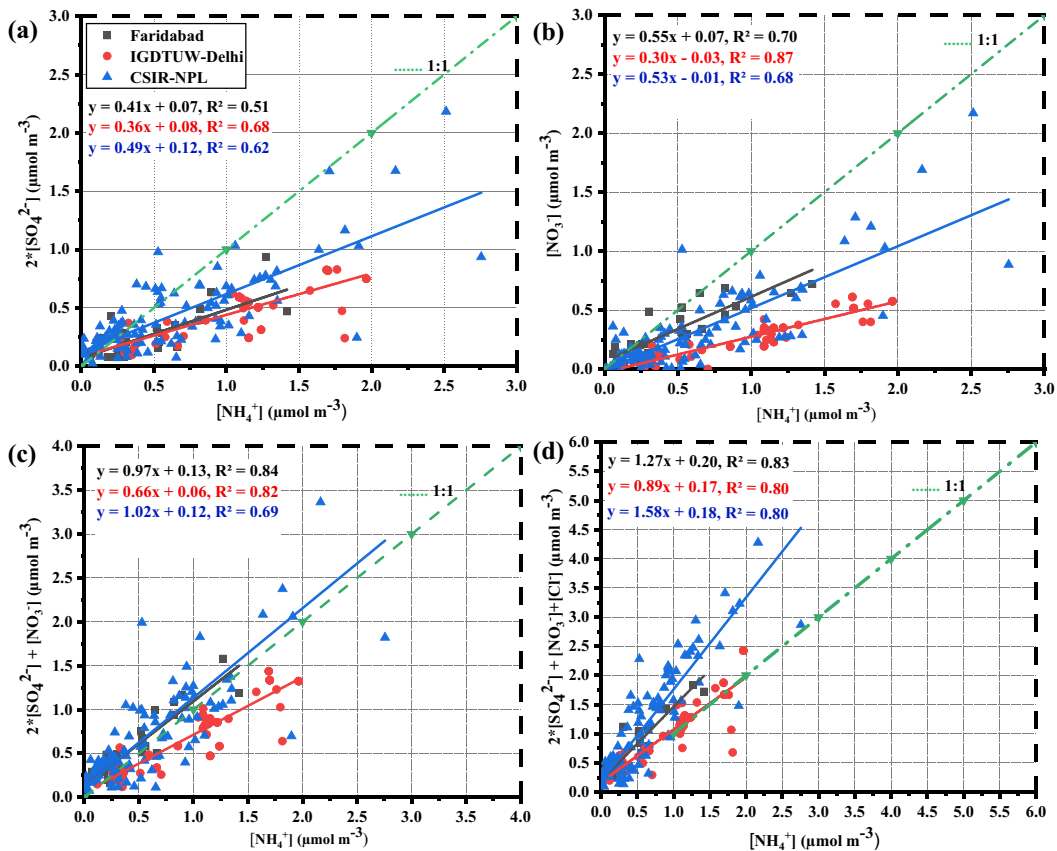


Fig. 2 Charge balance. **a** $[\text{NH}_4^+]$ vs $2^*[\text{SO}_4^{2-}]$. **b** $[\text{NH}_4^+]$ vs $[\text{NO}_3^-]$. **c** $[\text{NH}_4^+]$ vs $2^*[\text{SO}_4^{2-}] + [\text{NO}_3^-]$. **d** $[\text{NH}_4^+]$ vs $2^*[\text{SO}_4^{2-}] + [\text{NO}_3^-] + [\text{Cl}^-]$ of PM_{10}

Table 1. Over Faridabad, the concentration of Ca ($7.4 \pm 5.8 \mu\text{g m}^{-3}$) was found to be higher followed by Al ($5.9 \pm 2.3 \mu\text{g m}^{-3}$), S ($4.5 \pm 2.9 \mu\text{g m}^{-3}$), K ($4.4 \pm 4.9 \mu\text{g m}^{-3}$), Fe ($4.3 \pm 2.9 \mu\text{g m}^{-3}$) and Cl ($4.3 \pm 4.2 \mu\text{g m}^{-3}$) respectively. For IGDTUW-Delhi, Ca ($9.7 \pm 6.4 \mu\text{g m}^{-3}$) showed the higher concentration with Al ($5.3 \pm 3.6 \mu\text{g m}^{-3}$), Fe ($4.9 \pm 3.9 \mu\text{g m}^{-3}$), S ($4.6 \pm 3.2 \mu\text{g m}^{-3}$) and K ($4.0 \pm 2.7 \mu\text{g m}^{-3}$), respectively. Over CSIR-NPL, the concentration profile for elements were recorded as Ca ($7.4 \pm 3.6 \mu\text{g m}^{-3}$), Cl ($6.0 \pm 4.2 \mu\text{g m}^{-3}$), S ($5.0 \pm 2.1 \mu\text{g m}^{-3}$) and K ($4.1 \pm 2.2 \mu\text{g m}^{-3}$), respectively which reflected the dominance of the crustal elements over the heavy elements for all the three sites. Moreover, taking the average of the crustal elements (Ca, Mg, K, Mn, Al, Ti, Fe and Na) and the corresponding total mass concentration for each observation site, the crustal elements percentage is calculated, i.e. the crustal elements correspond to Faridabad, IGDTUW-Delhi and CSIR-NPL contributed as 12.2%, 8% and 11% to the PM_{10} concentration. Parallel studies like Jain et al. (2020) and Bawase et al. (2021) reported 14.1% and 11–21% of the crustal elements to PM_{10} . The spectral distribution (intensity vs 2θ) of the elements is enclosed in the supplementary study S1 (Figure S1; in supplementary information). Moreover, Fig. 3 shows a significantly positive correlation among the crustal elements (i.e. Al vs Mg, Ca, Ti and Fe) for Faridabad, IGDTUW-Delhi and CSIR-NPL: Mg vs Al ($R^2=0.72$, $R^2=0.86$, $R^2=0.89$), Ca vs Al ($R^2=0.78$, $R^2=0.67$, $R^2=0.77$), Ti vs Al ($R^2=0.60$, $R^2=0.62$, $R^2=0.86$) and Fe vs Al ($R^2=0.73$, $R^2=0.95$, $R^2=0.81$), respectively, thus emulating the profusion of mineral dust over the sites of Delhi-NCR. Additionally, for the locations Faridabad, IGDTUW-Delhi and CSIR-NPL, the ratios were calculated as Mg/Al (0.21, 0.25, 0.26) with range 0.1–1.0, 0.1–0.5 and 0.1–0.3 which are adjacent to the upper continental crust (UCC) value (Mg/Al, 0.17) (Taylor and McLennan, 1995). Ca/Al (1.0, 1.9, 1.2) with range 0.1–1.7, 1.0–6.1 and 0.5–2.1 which are quite higher than the UCC values (Ca/Al, 0.37). Fe/Al (0.6, 0.9, 0.5) with range 0.03–1.1, 0.6–1.4 and 0.01–1.05 which are fairly close to the UCC (Fe/Al, 0.43) (Taylor and McLennan, 1995). The higher values of the ratio Ca/Al and Fe/Al signify that the observation sites are enriched in Ca and Fe. Srinivas et al. (2011) reported Fe/Al,

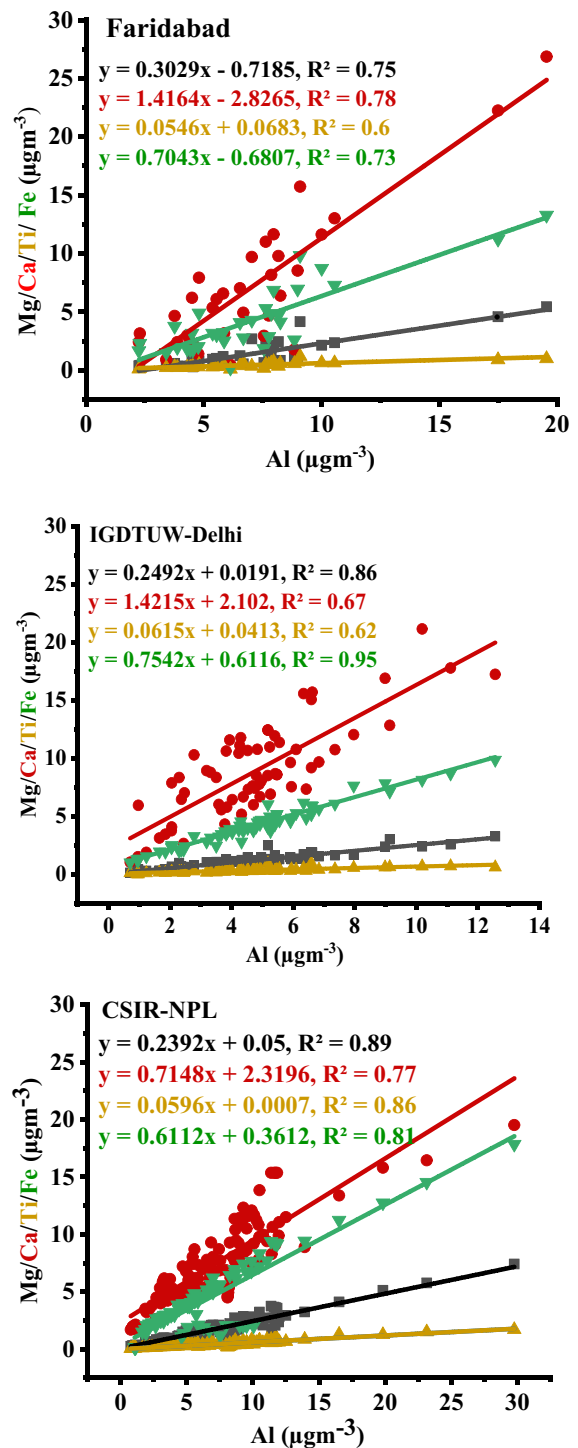


Fig. 3 Relationships (Al vs Mg, Ca, Ti, Fe) among the crustal/mineral/dust elements of PM_{10} over the three study sites

0.42; Ca/Al, 0.27; and Mg/Al, 0.24 across Bay of Bengal. Sharma et al. (2020) quantified Fe/Al, 1.07 and Ca/Al, 1.36. Fe/Al, 0.59 was reported at Nainital (Kumar & Sarin, 2009). For North Indian Plains, Fe/Al ranged 0.55–0.63 (Sarin et al., 1979). Recently, Sharma and Mandal (2023) also reported the similar sources of particulate matter over Delhi base on long-term monitoring.

Enrichment factor (EF)

To comprehend the root of the above analysed elements (e.g. crustal, natural or anthropogenic), EF is demarcated into ranges; elements with $EF < 5$ are classified as crustal or natural origination, $5 < EF < 10$ are mostly anthropogenic and natural, and elements with $EF > 10$ are considered as purely anthropogenic nature (Sharma et al., 2014, 2021; Sharma & Mandal, 2023; Jain et al., 2020). The annual EF for the study sites is represented in Fig. 4. Homogeneity in the sites (Faridabad, IGDTUW-Delhi and CSIR-NPL) resulted in analogous pattern of EF over the study sites. The elements (Ca, Mg, K, Mn, Al, Ti, Fe, Na) showed lower $EF < 5$, which accredited the crustal/soil dust. Elements (Mo, Zn, Cu, Cr, Pb, Ni) reflected $EF > 10$ or higher EF attributed to the anthropogenic sources. Study over Delhi (Sharma et al., 2021) reported similar pattern of lower EF (Al, Mg, Ti, Fe, Ca and K) and higher EF (Cr, Cu, Zn, Mo, Pb and Ni). The seasonal

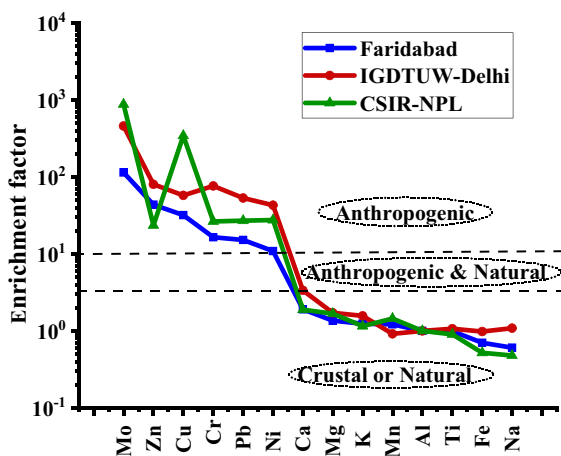


Fig. 4 Enrichment factor of elements in PM_{10} at the study sites

EF pattern for the three sites is presented in Figure S2 (see the supplementary information).

Morphology

Backscattered electron from the elastic collision comprehends the surface information (shape and size etc.) (Biswas et al., 2021). Morphological study of PM was done to grasp the idea about the possible sources towards the PM. The measurement scale for FE-SEM instrument is $10\ \mu\text{m}$ for the resolution range $\times 1100$ – 3000 , $1\ \mu\text{m}$ for $\times 3000$ – $30,000$ and $100\ \text{nm}$ for greater than $\times 30,000$ resolutions. Figure 5 shows that at a lower resolution ($\times 1500$, $10\ \mu\text{m}$), the morphology was homogenous and difficult to singularize the shape, and at higher resolution ($\times 3000$, $1\ \mu\text{m}$), distinct morphology of the PM was observed. Figure S3 represents the morphology corresponding to $\times 33,000$, $100\ \text{nm}$, i.e. $0.1\ \mu\text{m}$ for the three study sites. Blank in Fig. 5 represents the morphology of the quartz filter before sampling (i.e. no deposition). Pragmatic morphologies were analogous across the study sites (Table 2). In Fig. 5, morphologies of the PM at Faridabad and IGDTUW-Delhi were observed as spherical/fly ash, irregular and flocculent shaped, whereas at CSIR-NPL, irregular and flocculent types of morphologies were imaged. Spherical or the coal fired fly ash particulate is generally instigated from the incineration activities, high temperature combustions and biomass burning with the elemental composition (K, Al, Na, Mg etc.) (Zeb et al., 2018). Fe, Mn, Al etc. are the elemental compositions towards the irregular particulates, which are usually initiated through the crustal/soil dust and are typically wind-blown (Pipal et al., 2011). Flocculent particulates are basically cluster of spherical particulates of 30 – 50 -nm size, and they are primarily emanated through vehicles (Yin et al., 2020). Such sorts of particulate morphologies over the study sites are fairly acceptable as the sites are hedged with traffic flow, land fields, incineration activities, small-large-scale industries etc. A study sponsored by Delhi Pollution Control Committee (DPCC) imaged the fly ash, soil dust and aluminosilicate's particulate across the IIT-Delhi, Okhla, Murthal, Punjabi Bhag and Anand Vihar of Delhi (Shiva Nagendra and Khare, 2019). Pipal et al. (2011) found irregular, fine rod, crystalline and spherical types of particulate morphologies at Agra. Moreover, for the better understanding of the identification

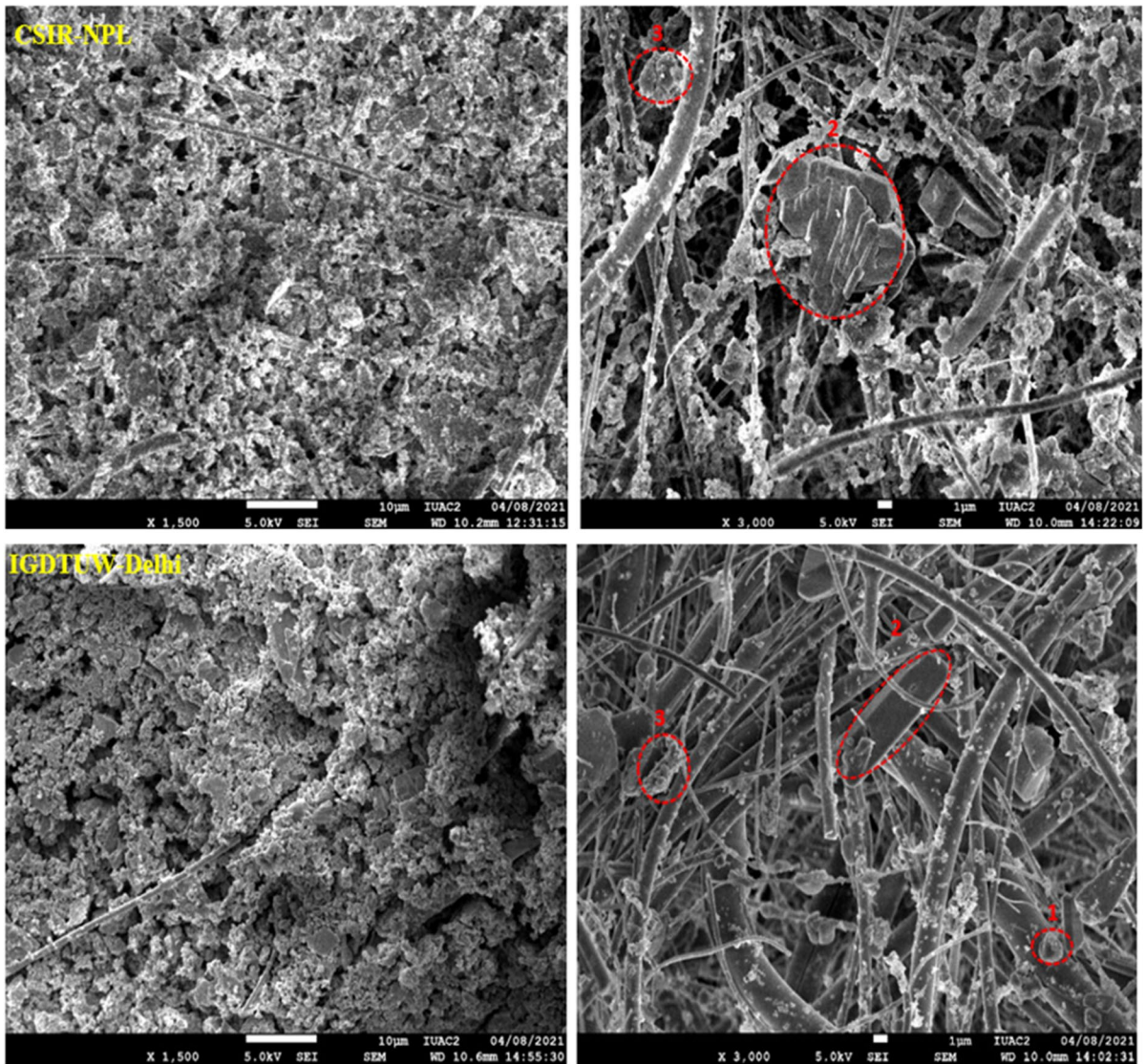


Fig. 5 SEM lower and higher resolution images reflecting the morphology of PM₁₀ for the three locations of NCR

and quantification of sources, the statistical approach is performed in the following section, where the two approaches (PMF and PCA) are applied.

Sources and possible regions of PM₁₀

In this study, the receptor models PMF (I-approach) and PCA (II-approach) have been applied to the species of PM₁₀ accordingly to categorize the sources and their contribution towards the ambient atmosphere of the locations. Furthermore, CBPF was performed to distinguish the local source regions.

Ist-approach (PMF)

Both the concentrations and the uncertainty files were measured as an elementary input to the PMF model. Assorted runs were made with the three-error estimation (EE) methods (BS, DISP, BS-DISP) to accomplish the optimal solution for individual location. PMF to the species of PM₁₀ at Faridabad, IGDTUW-Delhi, CSIR-NPL is summarized in Table 3 and Table S1–S2 (in supplementary information). BS was proceeded to comprehend the imitated base solution by mapping

Table 2 Morphological study at the study sites of NCR

Parameters	Faridabad	IGDTUW-Delhi	CSIR-NPL
Deposition	PM ₁₀	PM ₁₀	PM ₁₀
Sample ID	FBD-23	IT-01	NPL-05
Resolution	× 1500, × 3000	× 1500, × 3000	× 1500, × 3000
Size	10 μm, 1 μm	10 μm, 1 μm	10 μm, 1 μm
Scanning	Raster	Raster	Raster
Morphology	Spherical (1), irregular (2), flocculent (3)	Spherical (1), irregular (2), flocculent (3)	Irregular (2), flocculent (3)
Possible sources	Incineration activities, road dust, industrial and vehicular emissions	Incineration activities, road dust, industrial and vehicular emissions	Road dust, industrial and vehicular emissions
Elemental composition (XRF)	Na, Mg, Al, P, S, Cl, K, Ca, Ti, Cr, Mn, Fe, Ni, Cu, Zn, Mo, Pb, Ba	Na, Mg, Al, P, S, Cl, K, Ca, Ti, Cr, Mn, Fe, Ni, Cu, Zn, Mo, Pb, Ba	Na, Mg, Al, P, S, Cl, K, Ca, Ti, Cr, Mn, Fe, Ni, Cu, Zn, Mo, Pb, Ba

Table 3 PMF summary for the PM₁₀ over the study sites

Parameters	Faridabad	IGDTUW-Delhi	CSIR-NPL
<i>N</i> -species	25	25	29
<i>N</i> -samples	34	67	116
<i>Q</i> _{expected}	850	1675	3364
<i>Q</i> _{true}	1143	1477	2810
<i>Q</i> _{robust}	989	1445	2770
<i>Q</i> _{true} / <i>Q</i> _{expected}	3	2	2
Converged	Yes	Yes	Yes
Robust mode	Yes	Yes	Yes
S/N	Bad (Ba), weak (Ca ²⁺)	Weak (OC, WSOC, F-)	Weak (EC, Mn, Na ⁺)
Modelling uncertainty	7%	5%	8%
Number of iterations	100	100	100
Number of factors	6	6	6
Seed number	Random (48)	Random (94)	Random (11)
Selected base run	99	12	10
Block size	4	3	3
Number of BS run	100	100	100
Correlation <i>R</i> ²	0.6 <	0.6 <	0.6 <
DISP swaps	0	0	0
DISP active parameters	All	All	All
DISP dQ (max)	(4,8,12,32)	(4,8,12,32)	(4,8,12,32)

BS factor to base solution. In this way, BS resample the input point. In the present study, BS factor presented 100% of mapping with the base solution with model uncertainty (7% for Faridabad, 5% for IGDTUW, 8% for CSIR-NPL), signal to noise ratio ($S/N > 2$) and regression coefficient ($R^2 > 0.6$). Inflections in the swaps among the factor are vindicated by DISP; swapping of factors means there is exchange of features among the factor which is

not considered to define a well-defined solution (Paatero & Tapper, 1994a, 1994b; Brown et al., 2015). Current study performed zero swapping among the factors. BS-DISP pacts with the overall error of mapping, swapping, thus change in *Q* (Brown et al., 2015). With the consideration of EE, PMF model extracted 6-sources of PM₁₀ for each study site. Figure 6 represents the factor profile for individual site.

Faridabad

Source-I (soil dust): The first extracted source is soil dust (SD), as Al, Ti and Fe reflected the higher contribution (Fig. 6). This source contributed 15% to the PM₁₀ mass which agrees with the EF results in Fig. 4 as well the correlations in Fig. 3. Al, Ti, Fe, Ca, Na, Mg and K are framed as the marker components towards soil or road dust (Sharma & Mandal, 2023; Balachandran et al., 2000; Banerjee et al., 2015; Begum et al., 2011). Wind-blown local dust from the open field, constructions, re-suspended dust and the brick kiln stations in the vicinity of site could be the prime reason for such emission. Moreover, the long-range transport dust storm from the regions of Afghanistan and adjacent Pakistan in the north-west region contributes to the mass loading.

Source-II (unidentified): The second source is mixed/unidentified, as a single component Mn is contributing 12% of the PM₁₀ concentration. Mn is extant in diesel fuel and brake wear, whereas Mn, Ni and Cu are originated from industrial emissions (Jain et al., 2017). Quantification of source based on single component is quite baffling, thus considered as mixed/unidentified (Fig. 6).

Source-III (industrial emissions): Third source is identified as industrial emission (IE); the constituents (Cu, Zn, Br and Pb) contributed 14% of the PM₁₀ mass. Zn, Cu, Pb and Cr are defined as the marker to industries (small-large scaled) (Jain et al., 2020; Sharma et al., 2021; Gupta & Karar, 2007). As there are large- and small-scale manufacturing industries, e.g. steel, cotton, jute based, leather based, plastic and rubber, chemical, electrical machinery, wooden and agrobased are running in the new industrial town of Faridabad. Additionally, it also includes the major exportable manufacturers, i.e. shoes, tractor auto. Thus, emissions from such manufacturers could be the key sources for IE.

Source-IV (vehicular emissions): Fourth source is extracted as vehicular emission (VE); species (EC, WSOC, Cr, Mo) showed the higher influence to this factor. Sharma et al. (2021) reported EC, Cr, Zn, Mn and OC as source to vehicular emission. Studies (Gupta & Karar, 2007, Sharma et al., 2018, Sharma et al., 2021) quantified EC emission from diesel vehicle. It contributed around 19% to the

particulate mass. Toxic smoke emerging from the vehicles exhaust containing Cr dilutes the ambient air. Furthermore, the emissions from the non-exhaust as brake wear, tyre wear road surface wear and resuspended road dust enhance the VE.

Source-V (secondary aerosols): Fifth source, due to high contribution of (SO_4^{2-} , NO_3^- , NH_4^+), this source is classified as secondary aerosols (SA). SO_4^{2-} , NO_3^- and NH_4^+ in the atmosphere are ascribed by the gases (SO_2 , NO_x , NH_3) to particle conversions stimulated at higher and lower temperatures (Seinfeld, 1998, Sharma et al., 2015, Zheng et al., 2015; Song et al., 2006). SO_4^{2-} , NO_3^- and NH_4^+ are the key markers of secondary aerosols. Oxidation of NO_x at lower temperature results in the formation of secondary nitrate, whereas high temperature and the solar radiation favoured the formation of secondary sulphate via photochemical reactions. This source contributed approximately 23% to PM₁₀ mass.

Source-VI (sodium magnesium salt): Sodium magnesium salt (SMS) is the sixth source contributing 17% (Cl^- , Na^+ , Mg^{2+} and Ca^{2+}) in PM₁₀ concentration. Kothai et al. (2008) and Kumar et al. (2001) documented Na^+ , Cl^- , Mg^{2+} and Ca^{2+} as the precursors to sea salt and SMS. But in the present study, the sites are not in the vicinity of any coastal regions. Therefore, it is obvious to consider Na^+ , Mg^{2+} and Ca^{2+} as the markers of SMS. The resolved sources for the site are pretty conceivable, as the site reflects an urban atmosphere, and its topography includes the land field, walled traffic flux, small-large industries and construction stations.

IGDTUW-Delhi

Source-I (soil dust): Al, Ti and Fe framed the first source as soil dust. Approximately 16% of PM₁₀ is affianced with such source. Al, Ca, Mg, Fe and Ni are classified as SD sources (Moreno et al., 2013; Chelani et al., 2008). Ca associates the resuspension of bare soil from the agriculture fields by local winds. Small agricultural field on the bank of Yamuna River, road suspended dust and the long-range transport dust boosts such sources at the site. In India, the elemental tracers Ca, Al, Si, Ti, Pb, Cu, Co, Cr, Mg and Ni have been used for such source identification (Chelani et al., 2008; Sharma

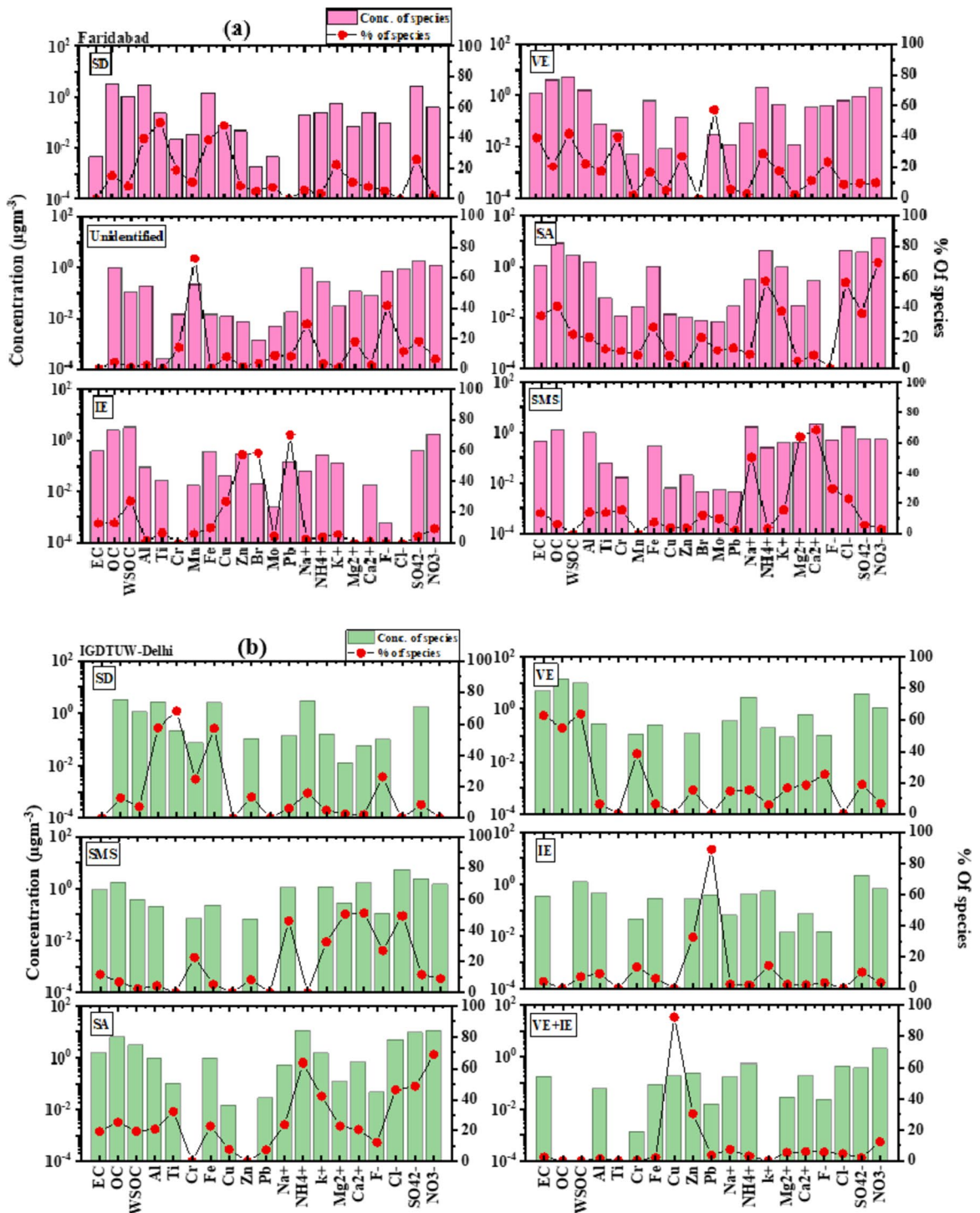


Fig. 6 PMF source profile of PM₁₀ for the observation sites (a Faridabad; b IGD TUW-Delhi; c CSIR-NPL)

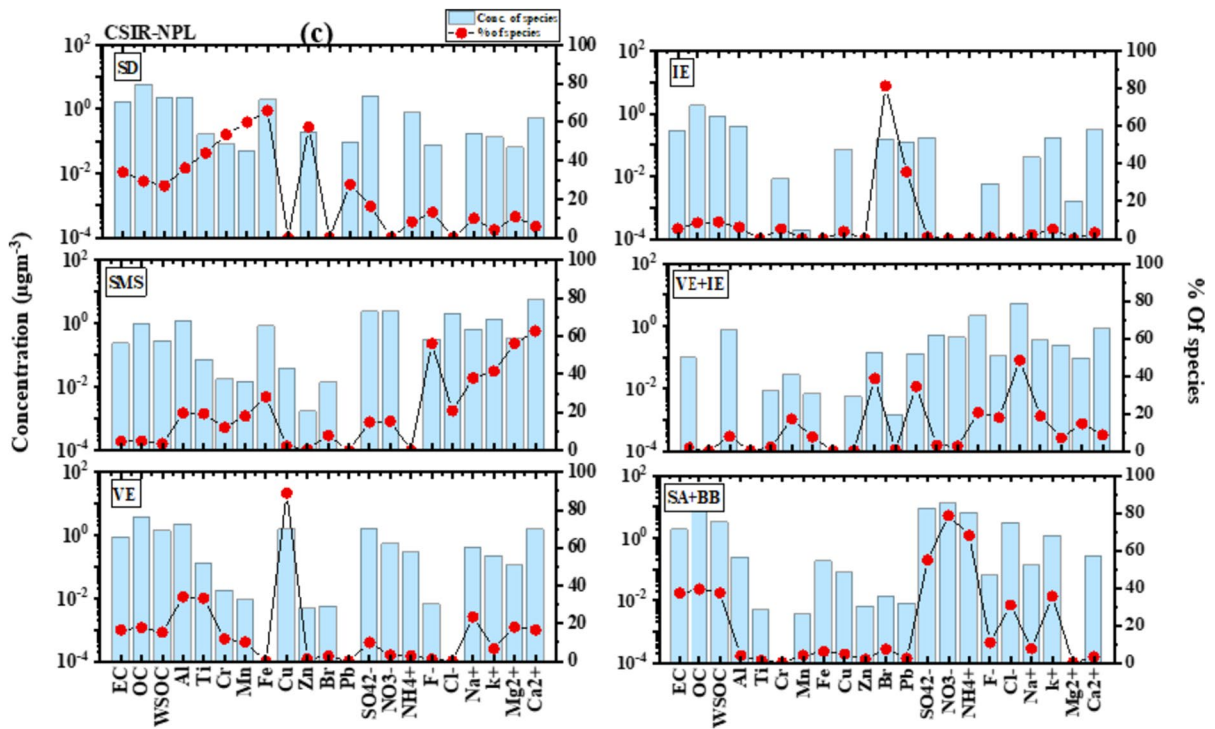


Fig. 6 (continued)

et al., 2015). Corresponding EF (Fig. 4) and the correlation (Fig. 3) results strengthen this result.

Source-II (sodium magnesium salt): Dominant contribution of Na^+ , Mg^{2+} , Cl^- and Ca^{2+} determined the source as sodium magnesium salt. The precursors Na^+ and Mg^{2+} with Cl^- and Ca^{2+} could have defined both the SMS and sea salt (SS) (Kumar et al., 2001), as the sites are not located nearby the coastal area, the SS contribution could be lesser, thus assumed as SMS. This has contributed around 18% to PM_{10} .

Source-III (secondary aerosols): High concentration of SO_4^{2-} , NO_3^- and NH_4^+ resulted in secondary aerosol. Around 27% of SA have subsidized to PM_{10} . It has been scrutinized that the secondary aerosols are being produced as $(\text{NH}_4)_2\text{SO}_4$ and NH_4NO_3 from the precursors (NO_x , SO_2 and NH_3) (Jain et al., 2018). Profusion of gases NO_x , SO_2 and NH_3 at Delhi supports such emissions over the site. Indian studies as Pant & Harrison (2012) and Khare & Baruah (2010) considered NH_4^+ as marker to biomass burning and SO_4^{2-} as coal combustion marker.

Source-IV (vehicular emissions): High values of EC, OC, WSOC and Cr outlined the source as vehicular emission. Pant & Harrison (2012) have considered EC, OC, Cr and Zn emissions from road vehicles. Silva et al. (2015) reported Cr and Zn from brake wear. International domain considers EC as marker to diesel exhaust marker, whereas in India, the VE tracers are generally Cu, Zn, Mn and Pb. As the site is walled with the running traffic roads also the railway tracks, residential areas and market place on the other side could be the possible sources for such emissions. VE have contributed 19% to the ambient PM_{10} at the site.

Source-V (industrial emissions): Species as Zn and Pb classified the source from Industrial emission. This source has 11% of contribution to PM_{10} at the location. Small-medium scaled industries in the vicinity of the site could be the possible reason for such emission. Jain et al. (2020) have reported Zn, Pb and Cr as industrial markers across Delhi. Such heavy elements might be instigated from the functioning small-medium-scale industries in the direction of study site.

Source-VI (vehicular + industrial emissions): Cu and Zn could be considered as the marker to both vehicular and industrial emissions. Cu is instigated through wearing of brake lining. Zn instigated as a tracer to electroplating, metallurgic and galvanising industries. Such amalgamated source has contributed 9% to the PM_{10} . Jain et al. (2017) have measured such species from vehicular, whereas Banerjee et al. (2015) and Sharma et al. (2021) defined the species to industrial emission. We note the small-scale industries and the heavy traffics, i.e. the busy inter-state bus terminal (ISBT), railway tracks, congested busy market place at a distance of few metres (<100 m) from the site. Such sources could be the foremost reason for the VE and IE kind of emissions at IGDTUW-Delhi.

CSIR-NPL

Source-I (soil dust): Profuse of Al, Ti, Fe, Mn and Zn framed the source as soil dust, which has contributed 24% to the ambient PM_{10} . Crustal elements (Al, Ca, Mg, Fe, Si, Ti and Na) are generally used as tracers for soil dust and are generally consistent in the upper continental crust composition (Sharma & Mandal, 2023; Sharma et al., 2021). SD not only associates with the mineral soil, but it also emerges from the activities as road dust, constructions, demolition works and other erosive process. The agricultural field (ICAR-Indian Agricultural Research Institute), central forest, busy traffic roads and residential areas possibly load the SD at the sampling site. Furthermore, the outcomes from the EF (Fig. 4) and the correlations (Fig. 3) supported this source. Sharma et al. (2016) have derived 20.5% contribution, and Jain et al. (2017) reported 20.5% of contribution to SD of PM_{10} in Delhi.

Source-II (sodium magnesium salt): This source has the 20% of contribution towards PM_{10} , as the tracers are found to be abundant as Na^+ , Mg^{2+} , Cl^- , F^- and Ca^{2+} . Cl^- , F^- and Na^+ are considered as the sea spray indicators. Long-range air parcel from Bay of Bengal and the Arabian sea could be the probable source, but the topography of the site CSIR-NPL reflects no coastal area in its vicinity. Parallel findings were reported in Sharma et al. (2016) with 21.3% contribution. Therefore, source is classified as SMS.

Source-III (vehicle emissions): High abundant of Cu with moderately Al premeditated the source as vehicular emissions. Gasoline and diesel vehicles can endorse the non-exhaust (compression) and exhaust (spark) emissions (Jain et al., 2017). Brake linings of vehicle assure the Cu emission. In Indian cities, the VE contribution may vary as 10–80% in atmospheric particulate (Sharma et al., 2016). This study estimated 15% of the VE contribution to atmospheric particulate (PM_{10}). Al may be originated from the soil dust. However, the contribution is moderate towards PM. Thus, defining the source as purely VE.

Source-IV (industrial emissions): Pb and Br inferred the factor as industrial emissions (IE). Approximately 8% of this source have a contribution to PM. Leaded fuel may be the indicator to Pb in atmospheric particulate at the sampling site. Pb is also emitted from acid-lead battery as well as other related industries (Jain et al., 2017).

Source-V (vehicular + industrial emissions): Species like Zn, Pb and Cl^- could be the possible sources for both vehicular and industrial emissions, thus their amalgamation. Twelve percent of the PM mass is portioned to this source. Pb with Cl^- may be attributed to coal combustion. Zn along with Pb attributes to IE as well VE.

Source-VI (secondary aerosol + biomass burning): Species SO_4^{2-} , NO_3^- , NH_4^+ , EC, OC, WSOC and K^+ are the possible markers to SA and BB. Around 21% of this amalgamation has contributed to PM_{10} at the site. Profusion of gases NO_x , SO_2 and NH_3 in Delhi results in the formation of SO_4^{2-} , NO_3^- and NH_4^+ . According to Wu et al. (2006), SO_4^{2-} along with K^+ has been defined as marker to wood, biomass burning. Pant & Harrison (2012) study over Asia and Europe considered K^+ as BB indicator. EC, OC and K^+ attribute to BB (Cesari et al., 2018). Jain et al. (2020) have showed 19% contribution of BB towards coarse mode (PM_{10}) concentration. PMF resolved sources are pretty conceivable for each individual site, as they reflect an urban atmosphere with the topography of land field, walled traffic flux, small-large industries, constructions, incineration activities etc.

Ind-approach (PCA)

PCA–Varimax rotation using the Kaiser normalization ($k > 0.6$) was modelled to the species of PM_{10} for the sites Faridabad, IGDTUW-Delhi and CSIR-NPL. The rotational matrix to the principal component is embedded in the Supplementary file S1 (Table 3 (a), (b), (c)).

Faridabad Figure 7 a represents the principal components (PCs) for 23 species of PM_{10} in Faridabad, PCA to such species built 5-components. In PC1, Na^+ and Mg^{2+} have showed a strongly positive loading value with a total variance of 35.3%. The species Na^+ and Mg^{2+} have been an active marker of sodium magnesium salt (SMS) as conferred above; thus, PC1 has been classified as SMS source. Moreover, it has contributed 11% to PM_{10} concentration. The second resolved source (PC2) is secondary aerosol + biomass burning (SA + BB), as the precursor of SA (SO_4^{2-} , NO_3^- , NH_4^+) and BB (OC, K^+ , Cl^-) has showed a strongly and moderately positive loading values with a total variance of 24.5%. This source contributes 30% to PM_{10} mass. Cl^- and K^+ are the sign for biomass burning (Shridhar et al., 2010; Khare & Baruah, 2010; Robinson et al., 2006; Pant & Harrison, 2012). PC3 is defined as soil dust; this source is supported by the crustal elements (Al, Ti, Fe and Cu) with strong positive loading values and the total variance of 9.4%. In addition, there %age contribution to particulate mass has estimated as approximately 36%. The PC4 has been classified as industrial emission, as Zn, Br and Pb represented strong loading values and Cu showed a moderately positive loading value. Furthermore, it showed 13% of contribution to particulate concentration. The total variance corresponding to this component is 7.9%. Amalgamation of industrial emission and vehicular emission (IE + VE) has been classified as PC5. The total variance to this factor is 5.6%. Mo, Cr and SO_4^{2-} figured a strong and moderate loading value. This has a contribution of 10% to PM.

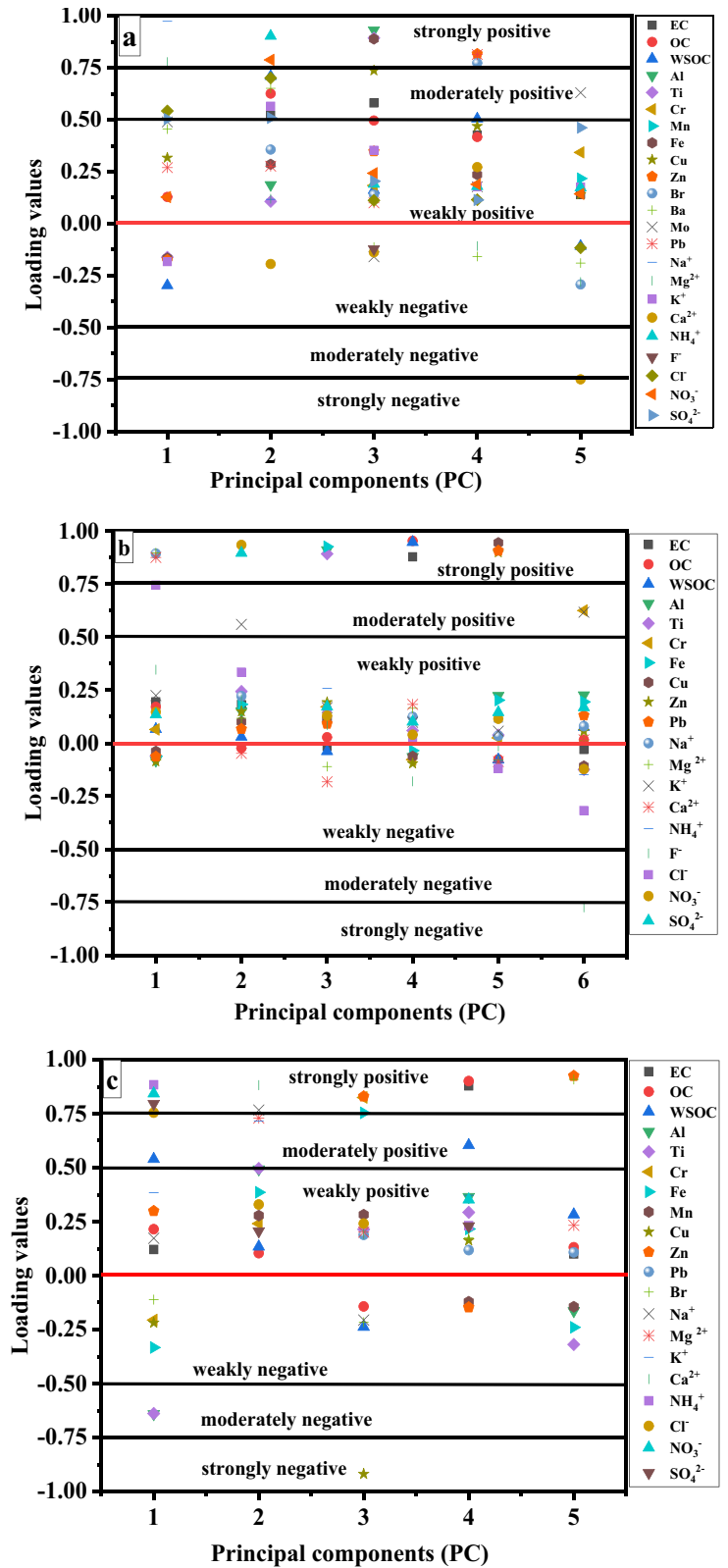
IGDTUW-Delhi PCA model was executed to 19 constituents of PM_{10} in IGDTUW-Delhi, such execution resulted in 6-components. As shown in Fig. 7 b, PC1 has been defined to SMS with a total variance of 17.18%. Na^+ , Mg^{2+} and Cl^- have been identified with strong positive loading factor (> 0.7). Additionally,

it has contributed 19.3% to PM_{10} concentration. The second component (PC2) has been defined as SA. SO_4^{2-} , NO_3^- and NH_4^+ imitated strong positive loading values with 16.8% of total variance, thus contributed in mass concentration by 4.7%. PC3 has assorted as SD, as Al, Ti and Fe reflected high loading value. The corresponding variance and the mass contributed have framed as 14.7% and 12.1%. High and strong positive loading factor of EC, OC and WSOC has delineated the source as amalgamation of VE and BB. Total variance is 14.3% and the mass contribution is 21.4%. Cu, Zn and Pb with the dominant loading factor outlined PC5 as VE. The last factor (PC6) has been identified as IE with the lowest variance of 8.89%. As the elements Cr and Al pointed moderately positive loading factor. Nearly, 14% of IE has contributed PM_{10} .

CSIR-NPL Modelled PCA to 20 species of PM_{10} extracted 5-PCs (Fig. 7 c), with different variances and contributions. PC1 has been classified as SA (SO_4^{2-} , NO_3^- , NH_4^+ and Cl^-), with 21.7% total variance. This species emanates in the range of strongly positive loading values. PC2 has inferred to the amalgamation of SMS and SD as Na^+ , Mg^{2+} , Ca^{2+} , Al, Ti, Fe and K^+ have been ranged to loading factor (> 0.5). Further with the variance of 16.9%, its contribution to PM_{10} is 23%. Strong loading factor with total variance of 16.29%, Cu, Fe and Zn have demarcated the source as IE (PC3). Moreover, 24% of IE has shared to PM. EC, OC, WSOC and K^+ with dominated loading factor resulted in BB source (PC4), with a total 12% contribution. PC5 described the amalgamation of IE and VE with a total variance of 10.4%. Zn and Br are the major loaded species. This amalgamated source has showed 7% of contribution to PM_{10} mass.

Observed/predicted concentration Observed data points correspond to the statistical calculated concentration, whereas the predicted data points are the model generated data points based on the input data file and the uncertainty (in PMF model). The observed values of the mass concentration (PM_{10}) have been regressed with the predicted data points for PM_{10} (Fig. 8). Exploring the PMF regression for the three locations, the observed and the predicted values showed a positive relation with $R^2 = 0.93$, $R^2 = 0.88$ and $R^2 = 0.94$ corresponding to Faridabad, IGDTUW-Delhi and CSIR-NPL respectively. The EE and the

Fig. 7 Rotational components factors resolved by PCA. **a** Faridabad. **b** IGDТУW-Delhi. **c** CSIR-NPL



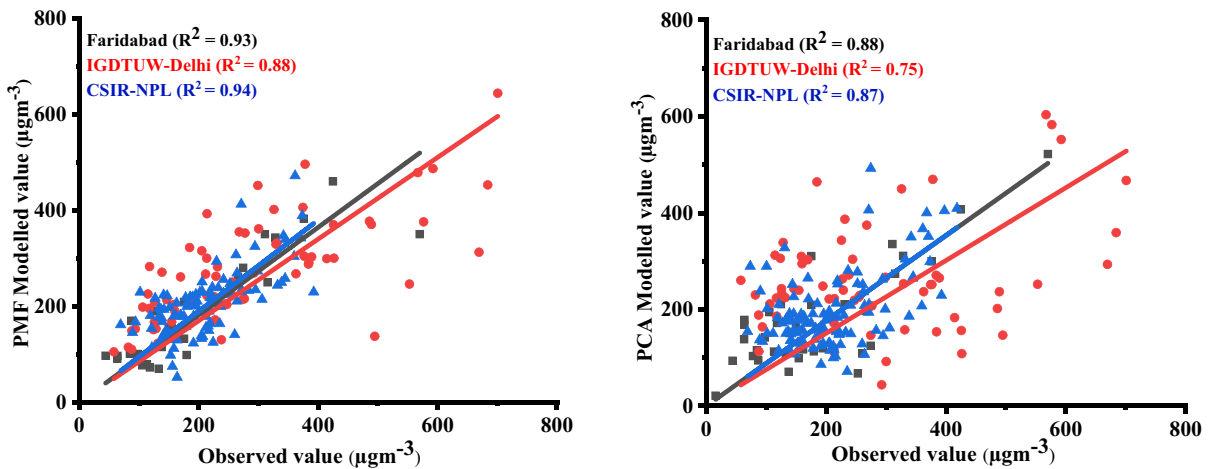


Fig. 8 Comparison of the modelled and the observed values of PM₁₀ for PCA and PMF receptor model

diagnoses in PMF were made incorporation with both observed and model generated data points. Likewise, Table 4, 5 and 6 represent the APCS-MLR regression of the observed and predicted concentration for individual species with $R^2 > 0.6$. 186 ± 123 ; 195 ± 121 , 256 ± 117 ; 275 ± 141 and 195 ± 77 ; $209 \pm 81 \mu\text{g m}^{-3}$ are the observed and modelled concentrations of PM₁₀ for Faridabad, IGDTUW-Delhi and CSIR-NPL respectively. Furthermore, Fig. 8 shows the positive correlation between the observed and predicted mass concentration (PM₁₀) with $R^2 = 0.88$, $R^2 = 0.75$ and $R^2 = 0.87$ corresponding to each site (Faridabad, IGDTUW-Delhi, CSIR-NPL). Such significant correlation among the observed and predicted/modelled mass concentration strengthened the outcomes of the model.

Outline to PMF and PCA

Both the model extracted the probable sources (SD, SMS, SA, BB, VE and IE) and the amalgamation of these sources (VE + BB, VE + IE, SMS + SD, SA + BB etc.) with different %age contribution to mass concentration of PM₁₀. Such extracted sources are quite obvious for the three urban sites of NCR-Delhi. Sampling sites at Faridabad are surrounded by the small-medium-scale industries, traffic junctions, agricultural/open fields, open incineration activities etc. IGDTUW-Delhi is curbed with the Inter State Bus Terminal (ISBT), the railway

junction and the small agricultural filed at the bank of Yamuna rivers. The traffic emission is quite high. Furthermore, it is surrounded with the residential and small-scale industries. CSIR-NPL is fenced with the heavy traffic junction, agricultural filed, forest and the residential areas (Banoo et al., 2020). In Delhi, Jain et al. (2017) made a comparable study using PMF (SA 25%, VE 13%, SD 16%, SMS 4%, IE, 11%). Sharma et al. (2016) identified SA 21.3%, SD 20.5%, VE 19.7%, BB 14.3%, FCC 13.7%, IE 6.2% and SS 4.3% using PMF.

Both PMF and PCA outlined a smooth outcome according to their performance and input requirement. The sources extracted by these methods are approximately similar. However, there is difference in the percentage contribution among the similar sources (Fig. 9). Different working mechanism, procedure or requirements could be the possible reason for such differences. In PCA/APCS, input data points are analysed by a statistical approach (Thurston & Spengler, 1985). PMF outcome is constructed by analysing and normalising each single data point (USEPA-PMF 2014). Values below detection limit (BDL) and the missing data point are prudently taken into account; along with the concentration file, it contemplates the uncertainty file (Jain et al., 2017). PMF perceives the rotational ambiguity and random error (USEPA-PMF 2014), which strengthened the outcomes of PMF model as compare to PCA (Banerjee et al., 2015; Jain et al., 2017).

Table 4 PCA-MLR summary for Faridabad

Species	SMS	SA+BB	SD	IE	IE+VE	Modelled value	Observed value	R ²
EC	0.11±0.23	0.92±0.81	2.34±2.23	0.28±0.26	1.17±0.91	4.81±2.52	4.85±3.58	0.82
OC	1.42±3.05	5.15±4.57	10.38±9.88	1.43±1.31	4.37±3.41	22.75±11.56	23.21±13.95	0.89
WSOC	-0.3±0.65	4.49±3.98	3.69±3.51	2.55±2.35	3.28±2.56	13.71±7.05	14.55±7.43	0.89
Al	0.1±0.22	0.67±0.59	3.6±3.43	0.63±0.58	1.15±0.9	6.15±3.61	6.98±3.66	0.82
Ti	-0.01±0.03	0.06±0.05	0.21±0.2	0.07±0.07	0.05±0.04	0.39±0.23	0.45±0.26	0.75
Cr	0.03±0.06	0.01±0.01	0.03±0.02	0.01±0.01	0.02±0.01	0.09±0.06	0.11±0.06	0.90
Mn	0.46±0.98	-0.04±0.04	0.02±0.02	0.02±0.02	-0.13±0.1	0.33±0.97	0.3±1.01	0.94
Fe	-0.26±-0.55	0.52±0.96	2.5±0.01	0.58±0.16	0.62±0.20	3.96±2.65	4.26±3.01	0.84
Cu	0.02±0.04	-0.02±0.02	0.1±0.09	0.05±0.04	0.01±0.01	0.16±0.11	0.17±0.14	0.80
Zn	-0.03±0.07	-0.04±0.04	0.17±0.16	0.28±0.26	0.23±0.18	0.59±0.38	0.61±0.49	0.81
Br	-	-	0.01±0.01	0.01±0.01	0.01±0.01	0.03±0.02	0.03±0.03	0.65
Ba	0.26±0.56	1.08±0.96	-0.01±0.01	-0.17±0.16	-0.27±0.21	0.9±0.98	0.87±1.18	0.83
Mo	0.01±0.02	0±0	0.01±0.01	0.01±0.01	0.02±0.01	0.05±0.03	0.06±0.02	0.79
Pb	0.03±0.05	0.02±0.02	0.04±0.04	0.09±0.08	0.02±0.02	0.2±0.11	0.2±0.15	0.79
Na ⁺	1.9±4.08	0.72±0.64	0.47±0.45	0.09±0.08	-0.19±0.15	3.0±4.0	3.2±4.3	0.88
Mg ²⁺	0.22±0.47	0.23±0.21	0.12±0.12	0.07±0.07	-0.02±0.01	0.63±0.48	0.73±0.67	0.65
K ⁺	0.01±0.03	0.83±0.74	1.01±0.96	0.88±0.81	0.02±0.02	2.76±1.51	3.06±2.03	0.73
Ca ²⁺	-0.29±0.62	0.31±0.28	0.35±0.33	0.45±0.42	2.46±1.92	3.29±2.16	3.72±3.36	0.62
NH ₄ ⁺	0.27±0.57	3.92±3.47	2.4±2.28	1.02±0.94	0.33±0.26	7.94±4.22	8.08±5.78	0.82
F ⁻	1.42±3.05	0.17±0.15	0.15±0.14	0.08±0.08	-0.07±0.05	1.76±3.01	1.87±3.13	0.88
Cl ⁻	1.72±3.68	3.57±3.16	2.15±2.04	0.87±0.8	-1.49±1.16	6.81±4.47	7.21±5.69	0.79
NO ₃ ⁻	2.17±4.65	7.39±6.55	7.19±6.84	2.49±2.29	-1.08±0.84	18.16±9.67	19.26±12.99	0.79
SO ₄ ²⁻	3.18±6.8	3.14±2.78	2.87±2.73	2.85±2.62	1.27±0.99	13.3±7.87	13.33±10.53	0.83
PM ₁₀	8.18±0.56	34.63±0.46	96.71±2.38	27.83±0.53	28.37±0.49	186±123	195±121	0.88

Table 5 PCA-MLR summary for IGDTUW-Delhi

Species	SMS	SA	SD	VE+BB	VE	IE	Modelled value	Observed value	R ²
EC	2.36±1.56	1.89±1.08	1.17±1.04	3.16±2.19	0.59±0.62	-0.31±0.26	8.85±3.06	9.42±5.17	0.76
OC	6.71±4.43	4.04±2.32	3.32±2.97	16.85±11.65	1.4±1.49	-2.74±2.22	29.58±12.81	30.84±19.3	0.79
WSOC	4.76±3.15	2.29±1.31	2.5±2.24	12.17±8.41	0.47±0.5	-2.07±1.68	20.13±9.14	21.31±14.34	0.75
Al	0.04±0.03	0.22±0.12	0.98±0.87	0.76±0.52	1.05±1.12	1.31±1.06	4.35±1.93	4.7±2.37	0.82
Ti	0.04±0.03	0.22±0.12	0.98±0.87	0.76±0.52	1.05±1.12	1.31±1.06	4.35±1.93	4.7±2.37	0.79
Cr	0.07±0.05	0.06±0.04	0.05±0.04	0.05±0.04	0.04±0.04	0.01±0.01	0.28±0.08	0.3±0.06	0.89
Fe	0.13±0.09	0.37±0.21	0.81±0.73	0.67±0.47	0.81±0.87	1.04±0.84	3.84±1.56	4.16±1.84	0.83
Cu	-0.07±0.04	0.03±0.02	0±0	-0.07±0.05	0.28±0.29	0.03±0.03	0.19±0.31	0.2±0.35	0.83
Zn	-0.01±0.01	0.06±0.04	0.06±0.05	-0.04±0.03	0.47±0.5	0.22±0.18	0.76±0.53	0.81±0.66	0.80
Pb	-0.16±0.11	0.1±0.06	-0.02±0.02	-0.07±0.05	0.48±0.51	0.15±0.12	0.48±0.54	0.5±0.67	0.74
Na ⁺	0.72±0.47	0.48±0.28	0.25±0.22	0.36±0.25	0.28±0.3	0.14±0.11	2.22±0.7	2.37±0.85	0.86
Mg ²⁺	0.23±0.15	0.13±0.07	0.05±0.04	0.08±0.05	0.05±0.05	-0.01±0.01	0.51±0.18	0.54±0.23	0.85
K ⁺	0.38±0.25	0.92±0.53	0.41±0.37	0.16±0.11	0.41±0.44	1.04±0.85	3.33±1.23	3.68±1.82	0.75
Ca ²⁺	1.06±0.7	0.86±0.49	0.38±0.34	0.66±0.45	0.29±0.31	-0.19±0.15	3.07±1.02	3.27±1.31	0.84
NH ₄ ⁺	2.24±1.48	5.57±3.19	2.48±2.22	-0.37±0.26	3.06±3.26	3.53±2.87	16.51±5.85	18.11±9.61	0.73
F ⁻	0.09±0.06	0.11±0.06	0.05±0.05	0.06±0.04	0.06±0.06	0.01±0.01	0.38±0.12	0.41±0.05	0.92
Cl ⁻	4.56±3.01	1.52±0.87	1.06±0.95	1.81±1.25	1.5±1.59	1.63±1.32	12.08±4.11	12.71±9.07	0.67
NO ₃ ⁻	1.44±0.95	8.21±4.71	2.21±1.98	-2.25±1.55	3.13±3.34	2.79±2.26	15.53±6.18	17.04±10.67	0.69
SO ₄ ²⁻	0.27±0.18	9.25±5.31	3.23±2.89	-0.64±0.44	2.85±3.03	4.4±3.57	19.35±7.32	21.2±11	0.75
PM ₁₀	53.64±35.43	17.47±10.02	28.27±25.31	52.3±36.15	93.74±99.79	45.21±36.69	256±117	275±141	0.75

Table 6 PCA-MLR summary for CSIR-NPL

Species	SA	SMS+SD	IE	BB	IE+VE	Modelled value	Observed value	R ²
EC	0.47±0.38	1.23±1.07	1.21±0.67	3.89±3	0.78±1.03	7.59±3.78	7.78±5.58	0.79
OC	4.33±3.43	4.29±3.74	5.34±2.95	7.63±5.88	2.89±3.8	24.48±10.16	25.45±13.4	0.85
WSOC	2.58±2.04	2.3±2	0.68±0.38	2.3±1.78	1.67±2.2	9.53±4.2	10.05±5.9	0.80
Al	0.94±0.74	0.61±0.53	4.91±2.71	0.27±0.21	0.46±0.61	7.18±3	7.08±4.48	0.86
Ti	0.07±0.05	0.07±0.06	0.31±0.17	0±0	-0.02±0.03	0.42±0.19	0.42±0.29	0.83
Cr	0.03±0.02	0.06±0.05	0.06±0.03	0±0	0±0	0.14±0.06	0.16±0.07	0.77
Fe	0.9±0.71	1.49±1.3	1.03±0.57	0.4±0.31	-0.6±0.79	3.22±1.8	3.32±3.31	0.62
Mn	0.02±0.02	0.08±0.07	0.01±0.01	0.07±0.05	-0.02±0.03	0.16±0.09	0.16±0.4	0.95
Cu	-0.34±0.27	-0.66±0.57	2.27±1.25	0.06±0.05	0.5±0.66	1.84±1.67	1.78±2.37	0.70
Zn	0.15±0.12	0.12±0.11	0.06±0.03	0±0	-0.04±0.06	0.29±0.17	0.36±0.24	0.62
Pb	0.12±0.1	0.08±0.07	-0.06±0.03	-0.04±0.03	0.22±0.29	0.32±0.29	0.37±0.34	0.76
Br	-0.01±0	0.04±0.03	-0.07±0.04	-0.04±0.03	0.26±0.35	0.18±0.34	0.19±0.36	0.90
Na ⁺	0.3±0.24	1.02±0.89	0.95±0.52	-0.24±0.18	0.11±0.14	2.14±1.03	2.12±1.66	0.78
Mg ²⁺	0.09±0.07	0.34±0.29	0.14±0.08	0.06±0.05	0±0	0.63±0.31	0.66±0.55	0.66
K ⁺	0.54±0.43	2.28±1.9	0.05±0.02	0.63±0.49	0.52±0.68	4.02±2.16	3.9±3.7	0.72
Ca ²⁺	0.31±0.25	4.67±4.07	2.91±1.61	1.06±0.82	-0.19±0.26	8.76±4.54	9.26±6.54	0.76
NH ₄ ⁺	7.32±5.8	2.77±2.42	-2.89±1.6	2.52±1.94	0.25±0.33	9.98±6.86	10.76±9.93	0.69
Cl ⁻	7.81±6.18	7.24±6.31	-5.63±3.11	4.09±3.15	-0.57±0.75	12.93±9.92	14.18±14.49	0.65
NO ₃ ⁻	18.5±14.66	4.98±4.34	-8.86±4.89	2.06±1.59	1.42±1.87	18.1±16.12	18.86±21.81	0.71
SO ₄ ²⁻	14.58±11.55	5.69±4.95	-4.64±2.57	1.77±1.36	1.58±2.09	18.98±12.78	20.15±16.59	0.77
PM ₁₀	42±33	34±30	48±27	53±41	17±23	195±77	209±81	0.87

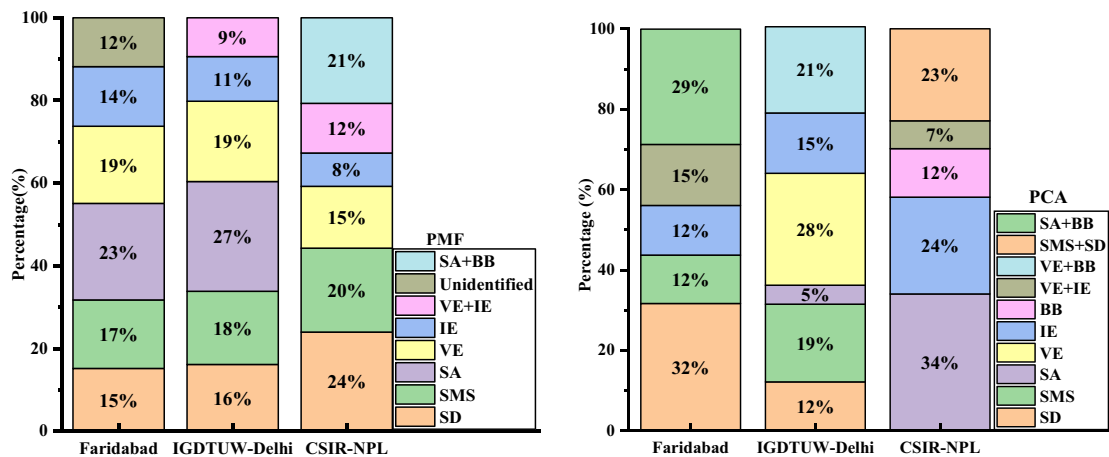


Fig. 9 Source percentage contribution profile of PM₁₀ extracted by PCA and PMF for the study sites of NCR

CBPF

Long-range transport of air parcel towards Delhi is dominated from North, North-West, North-East, South-West and South-East, i.e. sources in the region of Indo-Gangetic plain (IGP), Arabian sea and Bay

of Bengal, enhances the loading of atmospheric pollutants in Delhi (Banoo et al., 2020; Jain et al., 2020; Shivani et al., 2019). To grasp the directionality of the local source, CBPF plot is programmed as Fig. 10. The mass concentration of PM₁₀ is incorporated with the wind speed (ws) and the wind direction

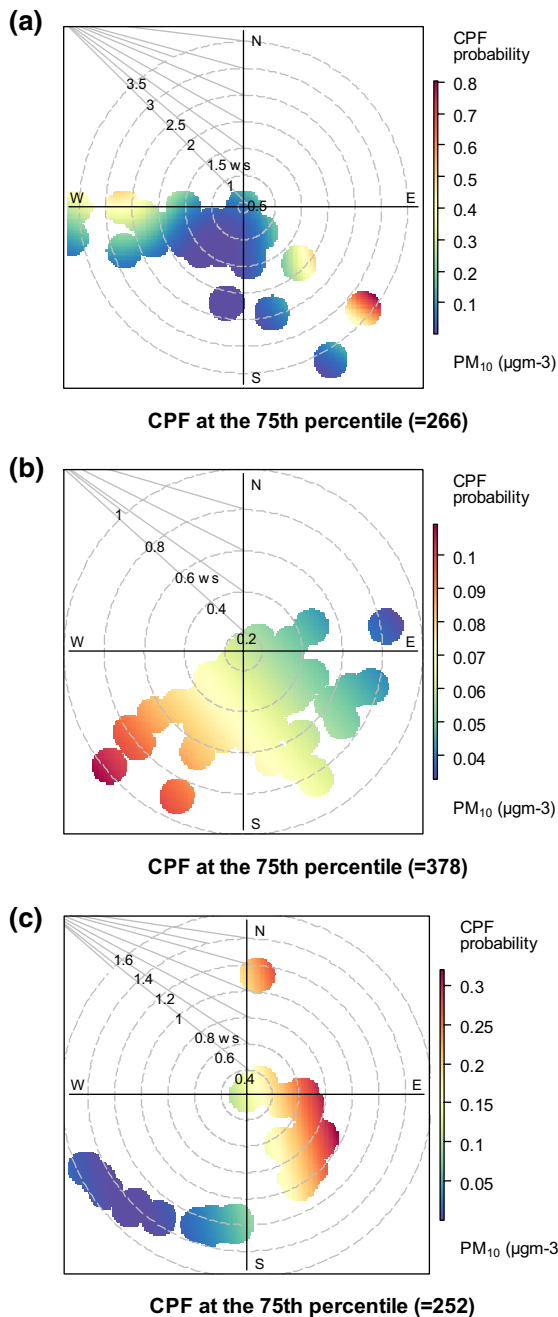


Fig. 10 CBPF plot of PM_{10} for the study sites. **a** Faridabad. **b** IGDTUW-Delhi. **c** CSIR-NPL

(wd) (Banoo et al., 2021). The dotted radial edges the ws. At Faridabad, the mass concentration (>75 th percentile), i.e. $266 \mu\text{g m}^{-3}$, was programmed with the ws ($0.4\text{--}3.7 \text{ ms}^{-1}$), which advocated the local source in the North-West (N-W), West-South (S-W) and the

South-East (S-E) regions of the receptor site aid in enhancing the mass concentration at the site. Moreover, the highly dense residential area, the agricultural field and the trivial traffic influx in the N-W and W-S including the national highway in the S-E direction of the receptor site could be the possible source emitter towards the site (Fig. 10 a). With (>75 th percentile) of mass concentration ($378 \mu\text{g m}^{-3}$) and the ws $\sim (0.1\text{--}1.0 \text{ ms}^{-1})$, CBPF for IGDTUW-Delhi directs the source in the local regions. W-S and S-E could be conceivable cause for mass loading at the site (Fig. 10 b). As the railway tracks, the dense fluxed traffic junctions (ISBT) including the dense residential area in the W-S (Banoo et al., 2020), Yamuna River bank (Gupta et al., 2018) and the small agricultural field in the S-W of the site could be the probable sources for the mass loading at the site. At CSIR-NPL, programmed ws $\sim (0.1\text{--}1.5 \text{ ms}^{-1})$ along with the mass concentration (>75 th, $252 \mu\text{g m}^{-3}$) proposed the sources in the N, N-E and S-W regions of the receptor site subsidize the mass concentration (Fig. 10 c). This contribution could be from the traffic, as the site is fenced with traffic junctions (Patel Nagar, Rajendar Place, Shadipur) in the N and N-W regions, agriculture field (ICAR-Indian Agricultural Research Institute) and forest (central ridge forest); moreover, the site is fenced with the residential areas (Banoo et al., 2021).

Conclusion

In this study, a whole array of chemical species (OC, EC, WOSC, Al, Ti, Na, Mg, Cr, Mn, Fe, Cu, Zn, Br, Ba, Mo Pb, F^- , Cl^- , SO_4^{2-} , NO_3^- , NH_4^+ , Na^+ , K^+ , Mg^{2+} , Ca^{2+}) were analysed and used for the identification and quantification of PM_{10} source over the three urban regions of NCR-Delhi using different approaches (EFs, morphology, PMF and PCA/APCS-MLR). Lastly, framed the CBPF for the directionality of local sources. The conclusions are enumerated as:

- It was observed that for over the observation sites, the mass concentrations of PM_{10} were quite higher than the NAAQS of India. The mass concentrations of PM_{10} were calculated as $195 \pm 121 \mu\text{g m}^{-3}$ over Faridabad, $275 \pm 141 \mu\text{g m}^{-3}$ for IGDTUW-Delhi and $209 \pm 81 \mu\text{g m}^{-3}$ over CSIR-NPL.

- Different types of morphological images (spherical, flocculent, irregular etc.) defined the possible source of PM₁₀ as biomass burning, road/soil dust, industrial and vehicular emission.
- Application of PMF to the particulate species over Faridabad extracted the factor SD (15%), IE (14%), VE (19%), SA (23%), SMS (17%) and unidentified source (12%). 6-sources were resolved for IGDTUW-Delhi, SD (16%), SMS (18%), SA (27%), VE (19%), IE (11%) and VE+IE (9%). Similarly, six factors correspond to CSIR-NPL, SD (24%), SMS (20%), VE (15%), IE (8%), VE + IE (12%) and SA + BB (21%). The observed and the predicted values showed a positive relation with $R^2=0.93$, $R^2=0.88$ and $R^2=0.94$ corresponding to Faridabad, IGDTUW-Delhi and CSIR-NPL, respectively.
- PCA/APCS-MLR resolved 5-sources at Faridabad, SMS (11%), SD (36%), IE (13%), SA + BB (30%) and IE + VE (10%) with different percentage of total variance. 6-sources at IGDTUW-Delhi, SMS (19%), SA (95%), SD (12%), VE (28%), IE (14%) and VE + BB (21%). At CSIR-NPL, it extracted 5-sources, SA (34%), SMS + SD (23%), IE (24%), BB (12%) and IE + VE (7%). Such sorts of sources are fairly acceptable for the three urban sites. Observed and the modelled concentration showed a positive correlation with $R^2=0.88$, $R^2=0.75$ and $R^2=0.87$ corresponding to each site (Faridabad, IGDTUW-Delhi, CSIR-NPL), respectively.
- CBPF programmed to Faridabad advocated the local source in the North-West (N-W), West-South (S-W) and the South-East (S-E) regions of the receptor site which aids in enhancing the mass concentration at the site. Source in the local regions of W-S and S-E could be conceivable cause for mass loading at the site IGDTUW-Delhi. At CSIR-NPL, the sources in the N, N-E and S-W regions subsidize the mass concentration at the site.

Acknowledgements The authors are thankful to the Director CSIR, NPL, New Delhi, and the Head, Environmental Sciences and Biomedical Metrology Division (ES&BMD), CSIR-NPL, New Delhi, India, for the encouragement and support. The authors thankfully acknowledge the Central Pollution Control Board (CPCB), New Delhi, India, for

metrological data (<https://cpcb.nic.in/>). The authors are thankful to IUAC for extending FE-SEM facility funded by the Ministry of Earth Sciences (MoES) under Geochronology project (MoES/P.O.(Seismic)8(09)-Geochron/2012).

Author contribution SKS: conceptualization, design of the study, funding acquisition, editing and review; the first draft was written by RB; data collection and analysis, editing and review were performed by RB, SG, RG, AD, NV, TKM and SKS; all the authors read, reviewed and approved the final manuscript.

Funding This study was funded by CSIR-National Physical Laboratory, New Delhi (OLP-210332).

Data availability The datasets developed during the current study are available from the corresponding author on reasonable request.

Declarations

Ethical approval All authors have read, understood and have complied as applicable with the statement on “Ethical responsibilities of Authors” as found in the Instructions for Authors.

Consent for publication All the authors have given their consent for the publication of this article and approved the final version of the manuscript.

Consent to participate Not applicable

Consent to publish Not applicable.

Competing interests The authors declare no competing interests.

References

- Adam, K., Greenbaum Daniel, S., Shaikh, R., Van Erp, A. M., & Russell, A. G. (2015). Particulate matter components, source, and health: Systematic approaches to testing effects. *Journal of the Air & Waste Management Association*, 65(5), 544–558. <https://doi.org/10.1080/10962247.2014.1001884>
- Andreae, M. O., & Merlet, P. (2001). Emission of trace gases and aerosols from biomass burning. *Glob Biogeochem Cycles*, 15, 955–966. <https://doi.org/10.1029/2000GB001382>
- Balachandran, S., Meena, B. R., & Khillare, P. S. (2000). Particle size distribution and its elemental composition in the ambient air of Delhi. *Environment International*, 26(1), 49–54. [https://doi.org/10.1016/s0160-4120\(00\)00077-5](https://doi.org/10.1016/s0160-4120(00)00077-5)
- Banerjee, T., Murari, V., Kumar, M., & Raju, M. P. (2015). Source apportionment of airborne particulates through receptor modeling: Indian scenario. *Atmospheric Research*, 64, 167–187. <https://doi.org/10.1016/j.atmosres.2015.04.017>

- Banoo, R., Sharma, S. K., Gadi, R., Gupta, S., & Mandal, T. K. (2020). Seasonal variation of carbonaceous species of PM₁₀ over urban sites of National Capital Region of India. *Aerosol Science and Engineering*, 4(2), 111–123. <https://doi.org/10.1007/s41810-020-00058-2>
- Banoo, R.; Sharma, S.K.; Rani, M.; Mandal, T.K (2021). Source and source region of carbonaceous species and trace elements in PM₁₀ over Delhi, India. In *Proceedings of the 4th International Electronic Conference on Atmospheric Sciences*, 16–31 July 2021, MDPI: Basel, Switzerland, <https://doi.org/10.3390/ecas2021-10346>
- Bapna, M., Sunder Raman, R., Ramachandran, S., & Rajesh, T. A. (2013). Airborne black carbon concentrations over an urban region in western India-temporal variability, effects of meteorology, and source regions. *Environmental Science and Pollution Research International*, 20(3), 1617–1631. <https://doi.org/10.1007/s11356-012-1053-3>
- Bawase, M., Sathe, Y., Khandaskar, H., & Thipse, S. (2021). Chemical composition and source attribution of PM_{2.5} and PM₁₀ in Delhi-National Capital Region (NCR) of India: results from an extensive seasonal campaign. *Journal of Atmospheric Chemistry*, 78, 35–58.
- Begam, G. R., Vachaspati, C. V., Ahammed, Y. N., Kumar, K. R., Reddy, R. R., Sharma, S. K., Saxena, M., & Mandal, T. K. (2017). Seasonal characteristics of water-soluble inorganic ions and carbonaceous aerosols in total suspended particulate matter at a rural semi-arid site, Kadapa (India). *Environmental Science and Pollution Research*, 24(2), 1719–1734.
- Begum, B. A., Biswas, S. K., & Hopke, P. K. (2011). Key issues in controlling air pollutants in Dhaka Bangladesh. *Atmos Environ*, 45(40), 7705–7771. <https://doi.org/10.1016/j.atmosenv.2010.10.022>
- Belis, C. A., Karagulian, F., Larsen, B. R., & Hopke, P. K. (2012). Critical review and meta-analysis of ambient particulate matter source apportionment using receptor models in Europe. *Atmospheric Environment*, 69, 94–108. <https://doi.org/10.1016/j.atmosenv.2012.11.009>
- Biswas, R., Abhilash, S. R., Himanshi Gupta, G. R., Umaphathy, A. D., & Nath, S. (2021). Fabrication of thin 140,142Ce target foils for study of nuclear reaction dynamics. *Vacuum*, 188, 110159. <https://doi.org/10.1016/j.vacuum.2021.110159>
- Brown, Steven G., Eberly, S., Paatero, P., Norris, Gary A., 2015. Methods for estimating uncertainty in PMF solutions: Examples with ambient air and water quality data and guidance on reporting PMF results, *Science of The Total Environment*, 518–519. <https://doi.org/10.1016/j.scitotenv.2015.01.022>.
- Cesari, D., De Benedetto, G. E., Bonasoni, P., Busetto, M., Dinioi, A., Merico, E., Chirizzi, D., Cristofanelli, P., Donato, A., Grasso, F. M., & Marinoni, A. (2018). Seasonal variability of PM_{2.5} and PM₁₀ composition and sources in an urban background site in Southern Italy. *Science of the Total Environment*, 612, 202–213. <https://doi.org/10.1016/j.scitotenv.2017.08.230>
- Chelani, A. B., Gajghate, D. G., & Devotta, S. (2008). Source apportionment of PM₁₀ in Mumbai, India using CMB model. *Bull Environ Contami Toxicol*, 81(2), 190–195. <https://doi.org/10.1007/s00128-008-9453-2>
- Chow, J. C., Watson, J. G. (2002). Review of PM_{2.5} and PM₁₀ apportionment for fossil fuel combustion and other sources by the chemical mass balance receptor model. *Energy & Fuels*, 16(2), 222–260. <https://doi.org/10.1021/ef0101715>
- Chow, J. C., Watson, J. G., Chen, L. W. A., Arnott, W. P., & Moosmuller, H. (2004). Equivalence of elemental carbon by thermal/optical reflectance and transmittance with different temperature protocols. *Environmental Science & Technology*, 38, 4414–4422.
- CPCB (208–2019). Annual report.
- Dall'Osto, M., Querol, X., Amato, F., Karanasiou, A., Lucarelli, F., Nava, S., Calzolari, G., Chiari, M., 2013. Hourly elemental concentrations in PM 2.5 aerosols sampled simultaneously at urban background and road site during SAPUSS–diurnal variations and PMF receptor modelling. *Atmospheric Chemistry and Physics*, 13(8), 4375–4392. [10.5194/acp-13-4375-2013](https://doi.org/10.5194/acp-13-4375-2013)
- Feng, X., Feng, Y., Chen, Y., Cai, J., Li, Q., & Chen, J. (2022). Source apportionment of PM_{2.5} during haze episodes in Shanghai by the PMF model with PAHs. *Journal of Cleaner Production*, 330, 0959–6526. <https://doi.org/10.1016/j.jclepro.2021.129850>
- Friend, A. J., Ayoko, G. A., Jager, D., Wust, M., Jayaratne, E. R., Jamriska, M., & Morawska, L. (2013). Sources of ultrafine particles and chemical species along a traffic corridor: Comparison of the results from two receptor models. *Environmental Chemistry*, 10(1), 54–63. <https://doi.org/10.1071/EN12149>
- Fuzzi, S., Baltensperger, U., Carslaw, Decesari, Denier van der Gon, H., Facchini, M. C., Fowler, D., Koren, I., Langford, Lohmann, U., Nemitz, E., Pandis, S., Riipinen, I., Rudich, Y., Schaap M., Slowik, J.G., Spracklen, D.V., Vignati, E., Wild, M., Williams, M., and Gilardoni, S., 2015. Particulate matter, air quality and climate: Lessons learned and future needs. *Atmospheric Chemistry and physics*. (15), 8217–8299 <https://doi.org/10.5194/acp-15-8217-2015>
- Gaonkar, Cynthia, V., Kumar, A., Matta, V. M., & Kurian, S., 2020. Assessment of crustal element and trace metal concentrations in atmospheric particulate matter over a coastal city in the Eastern Arabian Sea. *Journal of the Air & Waste Management Association*, 70:1, 78–92 <https://doi.org/10.1080/10962247.2019.1680458>
- García, J.H., Li, W.W., Cárdenas, N., Arimoto, R., Walton, J., Trujillo, D., 2006. Determination of PM_{2.5} sources using time-resolved integrated source and receptor models. *Chemosphere*. Vol. 65(11), 2018–2027. <https://doi.org/10.1016/j.chemosphere.2006.06.071>
- Gargava, P., Chow, J. C., Watson, J. G., & Lowenthal, D. H. (2014). Speciated PM₁₀ emission inventory for Delhi India. *Aerosol and Air Quality Research*, 14(5), 1515–1526. <https://doi.org/10.4209/aaqr.2013.02.0047>
- Gianini, M. F. D., Gehrig, R., Fischer, A., Ulrich, A., Wichser, A., & Hueglin, C. (2012). Chemical composition of PM₁₀ in Switzerland: An analysis for 2008/2009 and changes since 1998/1999. *Atmospheric Environment*, 54, 97–106. <https://doi.org/10.1016/j.atmosenv.2012.02.037>
- Gildemeister, A. E., Hopke, P. K., & Kim, E. (2017). Sources of fine urban particulate matter in Detroit, MI. *Chemosphere*, 69, 1064–1074. <https://doi.org/10.1016/j.chemosphere.2007.04.027>

- Gupta, A. K., & Karar, K. (2007). Source apportionment of PM₁₀ at residential and industrial sites of an urban region of Kolkata India. *Atmos Res*, 84(1), 30–41. <https://doi.org/10.1016/j.jhazmat.2006.08.013>
- Gupta, S., Gadi, R., Sharma, S. K., & Mandal, T. K. (2018). Characterization and source apportionment of organic compounds in PM₁₀ using PCA and PMF at a traffic hot-spot of Delhi. *Sustainable Cities and Society*, 38, 52–67. <https://doi.org/10.1016/j.scs.2018.01.051>
- Gupta, S. K., & Elumala, S. P. (2017). Size segregated particulate matter and its association with respiratory deposition doses among outdoor exercisers in Dhanbad City, India. *Journal of the Air & Water Management*, 67, 1137–1145. <https://doi.org/10.1080/10962247.2017.1344159>
- Guttikunda, S. K., Goel, R., & Pant, P. (2014). Nature of air pollution, emission sources, and management in the Indian cities. *Atmospheric Environment*, 95, 501–510. <https://doi.org/10.1016/j.atmosenv.2014.07.006>
- Henry, R. C., & Kim, B. M. (1990). Extension of self-modeling curve resolution to mixtures of more than three components: Part 1. Finding the basic feasible region. *Chemometrics and Intelligent Laboratory Systems*, 8, 205–216. [https://doi.org/10.1016/0169-7439\(90\)80136-T](https://doi.org/10.1016/0169-7439(90)80136-T)
- Hopke, P.K., (2016). A review of receptor modeling methods for source apportionment. *Journal of the Air & Waste Management Association* <https://doi.org/10.1080/10962247.2016.1140693>
- Hopke, P. K., Ito, K., Mar, T., Christensen, W. F., & Eatough, D. J. (2006). PM source apportionment and health effects: Intercomparison of source apportionment results. *Journal of Exposure Science and Environmental Epidemiology*, 16(3), 275–286. <https://doi.org/10.1038/sj.jea.7500458>
- Jain, S., Sharma, S. K., Choudhary, N., Masiwal, R., Saxena, M., Sharma, A., Mandal, T. K., Gupta, A., Gupta, N. C., & Sharma, C. (2017). Source apportionment of PM₁₀ in Delhi, India using PCA/APCS, UNMIX and PMF. *Environment Science and Pollution Research*, 24(17), 14637–14656. <https://doi.org/10.1007/s11356-017-8925-5>
- Jain, S., Sharma, S. K., Srivatava, M. K., Chaterjee, A., Singh, R. K., Mandal, T. K., & Saxena, M. (2018). Source apportionment of PM₁₀ over three tropical urban atmospheres at Indo-Gangetic Plain of India: An approach using different receptor models. *Environment Contamination and Toxicology*, 76, 114–128. <https://doi.org/10.1007/s00244-018-0572-4>
- Jain, S., Sharma, S.K., Vijayan, N., Mandal, T.K., 2020. Seasonal characteristics of aerosols (PM_{2.5} and PM₁₀) and their source apportionment using PMF: A four years study over Delhi, India. *Environ Poll*, 262: 114337. <https://doi.org/10.1016/j.envpol.2020.114337>
- Jolliffe, I.T., Cadima, J., 2016. Principal component analysis: A review and recent developments. *Philosophical Transactions of the Royal Society A: Mathematical, Physical and Engineering Sciences*, 374. <https://doi.org/10.1098/rsta.2015.0202>
- Khare, P., & Baruah, B. P., (2010). Elemental characterization and source identification of PM_{2.5} using multivariate analysis at the suburban site of north-east India. *Atmospheric Research*, 98(1), 148–162 <https://doi.org/10.1016/j.atmosres.2010.07.001>
- Kong, S. F., Ding, X., Bai, Z. P., Han, B., Chen, L., & Shi, J. W. (2010). A seasonal study of polycyclic aromatic hydrocarbons in PM_{2.5} and PM_{2.5-10} in five typical cities of Liaoning Province China. *Journal of Hazardous Materials*, 183, 70–80. <https://doi.org/10.1016/j.jhazmat.2010.06.107>
- Kothai, P., Saradhi, I. V., Prathibha, P., Hopke, P. K., Pandit, G. G., & Puranik, V. D. (2008). Source apportionment of coarse and fine particulate matter at Navi Mumbai India. *Aerosol and Air Quality Research*, 8(4), 423–436. <https://doi.org/10.4209/aaqr.2008.07.0027>
- Krudysz, M., Moore, K., Geller, M., Sioutas, C., & Froines, J. (2009). Intra-community spatial variability of particulate matter size distributions in Southern California/Los Angeles. *Atmospheric Chemistry and Physics*, 9, 1061–1075. <https://doi.org/10.5194/acp-9-1061-2009>
- Kumar, A. V., Patil, R. S., & Nambi, K. S. V. (2001). Source apportionment of sus-pended particulate matter at two traffic junctions in Mumbai India. *Atmospheric Environment*, 35(25), 4245–4251. [https://doi.org/10.1016/S1352-2310\(01\)002588](https://doi.org/10.1016/S1352-2310(01)002588)
- Kumar, A., & Sarin, M. M. (2009). Mineral aerosols from western India: Temporal variability of coarse and fine atmospheric dust and elemental characteristics. *Atmospheric Environment*, 43(26), 4005–4013. <https://doi.org/10.1016/j.atmosenv.2009.05.014>
- Lang, Y. H., Li, G. L., Wang, X. M., Peng, P., & Bai, J. (2015). Combination of Unmix and positive matrix factorization model identifying contributions to carcinogenicity and mutagenicity for polycyclic aromatic hydrocarbons sources in Liaohe delta reed wetland soils, China. *Chemosphere*, 120, 431–437. <https://doi.org/10.1016/j.marpolbul.2014.11.009>
- Larsen, R.K., Baker, J.E., 2003. Source apportionment of polycyclic aromatic hydrocarbons in the urban atmosphere: A comparison of three methods. *Environ Sci Technol*. 1;37(9):1873–81. <https://doi.org/10.1021/es0206184>
- Lima, Luiz and do Nascimento, Clístenes Williams Araújo and Silva, Fernando and Araújo, Paula 2022. Baseline concentrations, source apportionment, and probabilistic risk assessment of heavy metals in urban street dust in North-east Brazil. <https://doi.org/10.2139/ssrn.4206916>
- Liu, Y., Yan, C., Ding, X., Wang, X., Fu, Q., Zhao, Q., Zhang, Y., Duan, Y., Qiu, X., & Zheng, M. (2017). Sources and spatial distribution of particulate polycyclic aromatic hydrocarbons in Shanghai, China. *The Science of the Total Environment*, 584–585, 307–317. <https://doi.org/10.1016/j.scitotenv.2016.12.134>
- Mandal, P., Saud, T., Sarkar, R., Mandal, A., Sharma, S. K., & Mandal, T. K. (2014). High seasonal variation of atmospheric C and particle concentrations in Delhi India. *Environ Chem Lett*, 12(1), 225–230. <https://doi.org/10.1007/s10311-013-0438-y>
- Masiol, M., Squizzato, S., Cheng, M. D., Rich, D. Q., & Hopke, P. K. (2019). Differential probability functions for investigating long-term changes in local and regional air pollution sources. *Aerosol and Air Quality Research*, 19, 724–736. <https://doi.org/10.4209/aaqr.2018.09.0327>
- Moreno, T., Karanasiou, A., Amato, F., Lucarelli, F., Nava, S., Calzolari, G., Chiari, M., Coz, E., Artíñano, B., Lumberras, J., Borge, R., Boldo, E., Linares, C., Alastuey,

- A., Querol, X., & Gibbons, W. (2013). Daily and hourly sourcing of metallic and mineral dust in urban air contaminated by traffic and coal-burning emissions. *Atmospheric Environment*, 68, 33–44. <https://doi.org/10.1016/j.atmosenv.2012.11.037>
- Norris, G., Duvall, R., Brown, S., Bai, S., 2014. EPA positive matrix factorization (PMF) 5.0 fundamentals and user guide. Prepared for the, U.S. Environmental Protection Agency Office of Research and Development, Washington, DC (EPA/600/R-14/108; STI-910511–5594-UG, April).
- Ogundele, L. T., Owoade, O. K., Olise, F. S., & Hopke, P. K. (2016). Source identification and apportionment of PM_{2.5} and PM_{2.5–10} in iron and steel scrap smelting factory environment using PMF, PCFA and UNMIX receptor models. *Environmental Monitoring and Assessment*, 188(10), 574. <https://doi.org/10.1007/s10661-016-5585-8>
- Olson, D. A., & Norris, G. A. (2008). Chemical characterization of ambient particulate matter near the World Trade Centre: Source apportionment using organic and inorganic sources markers. *Atmospheric Environment*, 42, 7310–7315. <https://doi.org/10.1021/es030689>
- Paatero, P. (1997). Least squares formulation of robust non-negative factor analysis. *Chemometrics and Intelligent Laboratory Systems*, 37(1), 23–35. [https://doi.org/10.1016/S0169-7439\(96\)00044-5](https://doi.org/10.1016/S0169-7439(96)00044-5)
- Paatero, P., & Tapper, U. (1994a). Positive matrix factorization: A non-negative factor model with optimal utilization of error estimates of data values. *Environmetrics*, 5(2), 111–126. <https://doi.org/10.1002/env.3170050203>
- Pant, P., & Harrison, R. M. (2012). Critical review of receptor modelling for particulate matter: A case study of India. *Atmospheric Environment*, 49, 1–12. <https://doi.org/10.1016/j.atmosenv.2011.11.060>
- Pant, P., & Harrison, R. M. (2013). Estimation of the contribution of road traffic emissions to particulate matter concentrations from field measurements: A review. *Atmospheric Environment*, 77, 78–97. <https://doi.org/10.1016/j.ATMOSENV.2013.04.028>
- Pant, P., Shukla, A., Kohl, S. D., Chow, J. C., Watson, J. G., & Harrison, R. M. (2015). Characterization of ambient PM_{2.5} at a pollution hotspot in New Delhi, India and inference of sources. *Atmospheric Environment*, 109, 178–189. <https://doi.org/10.1016/j.atmosenv.2015.02.074>
- Paterson, K. G., Sagady, J. L., Hooper, D. L., Bertman, S. B., Carroll, M. A., & Shepson, P. B. (1999). Analysis of air quality data using positive matrix factorization. *Environmental Science & Technology*, 33(4), 635–641. <https://doi.org/10.1021/es980605j>
- Paul, C., Suman, A.A., Sultan., 2013. Methodological analysis of principal component analysis (PCA) method. *International Journal of Computational Engineering & Management*, 16, 32–38. <http://www.ijcem.org/>
- Pakbin, P., Hudda, N., Cheung, K. L., Katharine F., Moore & Constantino's Sioutas. (2010). Spatial and temporal variability of coarse (PM_{10–2.5}) particulate matter concentrations in the Los Angeles area. *Aerosol Science and Technology*, 44(7), 514–525. <https://doi.org/10.1080/02786821003749509>
- Paatero, P., Unto Tapper., 1994. Positive matrix factorization: A non-negative factor model with optimal utilization of error estimates of data values., 5(2), 111–126. <https://doi.org/10.1002/env.3170050203>
- Perrino, C., Tiwari, S., Catrambone, M., Dalla Torre, S., Rantica, E., & Canepari, S. (2011). Chemical characterization of atmospheric PM in Delhi, India, during different periods of the year including Diwali festival. *Atmospheric Pollution Research*, 2(4), 418–427. <https://doi.org/10.5094/APR.2011.048>
- Pipal, A. S., Kulshrestha, A., & Taneja, A. (2011). Characterization and morphological analysis of airborne PM_{2.5} and PM₁₀ in Agra located in north central India. *Atmospheric Environment*, 45(21), 3621–3630.
- Polissar, A. V., Hopke, P. K., Paatero, P., Malm, W. C., & Sisler, J. F. (1998). Atmospheric aerosol over Alaska: Elemental composition and sources. *Journal of Geophysical Research*, 103, 19045–19057. <https://doi.org/10.1029/98JD01212>
- Prakash, J., Lohia, T., & Mandariya, A. K. (2018). Chemical characterization and quantitative assessment of source-specific health risk of trace metals in PM_{1.0} at a road site of Delhi India. *Environ Sci Pollut Res*, 25, 8747–8764. <https://doi.org/10.1007/s11356-017-1174-9>
- Rai, P., Chakraborty, A., Mandariya, A. K., & Gupta, T. (2016). Composition and source apportionment of PM₁ at urban site Kanpur in India using PMF coupled with CBPF. *Atmospheric Research*, 178–179, 506–520. <https://doi.org/10.1016/j.atmosres.2016.04.015>
- Rizwan, S.A., Nongkynrih, Baridalayne., and Gupta, Sanjeev Kumar., 2013. Air pollution in Delhi. Its magnitude and effects on health. *Indian Journal of Community Medicine*, (38),1. <https://doi.org/10.4103/2F0970-0218.106617>
- Robinson, A. L., Subramanian, R., Donahue, N. M., Bernardo-Bricker, A., & Rogge, W. F. (2006). Source apportionment of molecular markers and organic aerosol. 2 Biomass Smoke. *Environmental Science & Technology*, 40, 7811–7819. <https://doi.org/10.1021/es060782h>
- Saad, M., Bibi, M., Masmoudi, M., Chevallier, S., & Alfaro, S. (2018). Compositional variability of the aerosols collected in Sfax (Central Tunisia). *Journal of Atmospheric and Solar - Terrestrial Physics*, 172, 53–62. <https://doi.org/10.1016/j.jastp.2018.03.011>
- Sarin, M. M., Borole, D. V., & Krishnaswami, S. (1979). Geochemistry and geochronology of sediments from the Bay of Bengal and the equatorial Indian Ocean. *Proceedings of the Indian Academy of Science*, 88, 131–154.
- Seinfeld, J., 1998. Atmospheric chemistry and physics: From air pollution to climate change.7:26–26. <https://doi.org/10.1080/00139157.1999.10544295>
- Sharma, S. K., & Mandal, T. K. (2023). Elemental composition and sources of fine particulate matter (PM_{2.5}) in Delhi, India. *Bulletin of Environmental Contamination and Toxicology*, 110, 60. <https://doi.org/10.1007/s00128-023-03707-7>
- Sharma, S. K., Mandal, T. K., Saxena, M., Sharma, A., & Gautam, R. (2014). Source apportionment of PM₁₀ by using positive matrix factorization at an urban site of Delhi, India. *Urban Climate*, 10, 656–670. <https://doi.org/10.1016/2Fj.uclim.2013.11.002>
- Sharma, S. K., Sharma, A., Saxena, M., Choudhary, N., Masiwal, R., & Mandal, T. K. (2015). Chemical characterization and source apportionment of aerosol at an urban area of central Delhi, India. *Atmospheric Pollution Research*, 7, 110–121. <https://doi.org/10.1016/j.apr.2015.08.002>

- Sharma, S. K., Mandal, T. K., Jain, S., Saraswati., Sharma, A., Saxena, M. (2016). Source apportionment of PM_{2.5} in Delhi, India using PMF model. *Bull Environ Contamin Toxicol* 97:286–293. <https://doi.org/10.1007/s00128-016-1836-1>
- Sharma, S. K., Mandal, T. K., Sharma, A., Jain, S., & Saraswati. (2018). Carbonaceous species of PM_{2.5} in megacity Delhi, India during 2012–2016. *Bulletin of Environmental Contamination and Toxicology*, 100, 695–701. <https://doi.org/10.1007/s00128-018-2313-9>
- Sharma, S. K., Choudhary, N., Srivastava, P., Naja, M., Vijayan, N., Kotnala, G., Mandal, T. K. (2020). Variation of carbonaceous species and trace elements in PM₁₀ at a mountain site in the central Himalayan region of India. *Journal of Atmospheric Chemistry*, 77(3), 49–62. <https://link.springer.com/article/https://doi.org/10.1007/s10874-020-09402-9>
- Sharma, S. K., Banoo, R., & Mandal, T. K. (2021). Seasonal characteristics and sources of carbonaceous components and elements of PM₁₀ (2010–2019) in Delhi India. *J Atmos Chem*, 78, 251–270. <https://doi.org/10.1007/s10874-021-09424-x>
- Shiva Nagendra, S. M., & Khare, M. (2019). Source apportionment of ambient particulate matter during winter season in Delhi, Report: Delhi Pollution Control Committee, Government of National Capital Region, New Delhi. <https://www.dpcc.delhigovt.nic.in>
- Shivani, S., Gadi, R., Saxena, M., Sharma, S.K., Mandal, T.K., 2019. Short term degradation of air quality during major firework events in Delhi, India. *Meteorol Atmos Phys* 131(4):753–764. <https://link.springer.com/article/https://doi.org/10.1007/s00703-018-0602-9>
- Shridhar, V., Khillare, P. S., Agarwal, T., & Ray, S. (2010). Metallic species in ambient particulate matter at rural and urban location of Delhi. *Journal of Hazardous Materials*, 175(1), 600–607. <https://doi.org/10.1016/j.jhazmat.2009.10.047>
- Shubhankar, B., & Ambade, B. (2016). Chemical characterization of carbonaceous carbon from industrial and semi urban site of the eastern India. *Springer plus*, 5, 837. <https://doi.org/10.1186/s40064-016-2506-9>
- Silva, M., Santos, M. G., Cooray, A., & Gong, Y. (2015). Prospects for detecting C II emission during the Epoch of reionization. *The Astrophysical Journal*, 806(2), 209.
- Song, Y., Xie, S., Zhang, Y., Zeng, L., Salmon, L. G., & Zheng, M. (2006). Source apportionment of PM_{2.5} in Beijing using principal component analysis/absolute principal component scores and UNMIX. *Science of the Total Environment*, 372(1), 278–286. <https://doi.org/10.1016/j.scitotenv.2006.08.041>
- Soleimani, M., Ebrahimi, Z., Mirghaffari, N., et al. (2022). Seasonal trend and source identification of polycyclic aromatic hydrocarbons associated with fine particulate matters (PM_{2.5}) in Isfahan City, Iran, using diagnostic ratio and PMF model. *Environmental Science and Pollution Research*, 29, 26449–26464. <https://doi.org/10.1007/s11356-021-17635-8>
- Taylor, S. R., & McLennan, S. M. (1995). The geochemical evolution of the continental crust. *Review of Geophysics*, 33(2), 241–265.
- Thurston, G. D., & Spengler, J. D. (1985). A quantitative assessment of source contribution in metropolitan Boston. *Atmospheric Environment*, 19, 257–259. [https://doi.org/10.1016/0004-6981\(85\)90132-5](https://doi.org/10.1016/0004-6981(85)90132-5)
- Tiwari, S., Pervez, S., Cinzia, P., Bisht, D.S., Kumar, A., Chate, D.M., 2013. Chemical characterization of atmospheric particulate matter in Delhi, India, part II: Source apportionment studies using PMF. *Sustain Environ Res* 23(5):295–306
- Uria-Tellaetxe, I., & Carslaw, D. C. (2014). Conditional bivariate probability function for source identification. *Environmental Modelling and Software*, 59, 1–9. <https://doi.org/10.1016/j.envsoft.2014.05.002>
- Wilson, J. G., Kingham, S., Pearce, J., & Sturman, A. P. (2005). A review of intraurban variations in particulate air pollution: Implications for epidemiological research. *Atmospheric Environment*, 39, 6444–6462. <https://doi.org/10.1016/j.atmosenv.2005.07.030>
- Wu, D., Tie, X., & Deng, X. (2006). Chemical characterizations of soluble aerosols in southern China. *Chemosphere*, 64(5), 749–757.
- Yin, D., Zhao, S., Qu, J., Yu, Y., Kang, S., Ren, X., Zhang, J., Zou, Y., Dong, L., Li, J. & He, J. (2020). The vertical profiles of carbonaceous aerosols and key influencing factors during wintertime over western Sichuan Basin, China. *Atmospheric Environment*, 223, 117269.
- Zeb, B., Alam, K., Sorooshian, A., Blaschke, T., Ahmad, I., & Shahid, I. (2018). On the morphology and composition of particulate matter in an urban environment. *Aerosol and Air Quality Research*, 18(6), 1431–1447. <https://doi.org/10.4209/aaqr.2017.09.0340>
- Zheng, B., Zhang, Q., Zhang, Y., He, K. B., Wang, K., Zheng, G. J., Duan, F. K., Ma, Y. L., & Kimoto, T. (2015). Heterogeneous chemistry: A mechanism missing in current models to explain secondary inorganic aerosol formation during the January 2013 haze episode in North China. *Atmospheric Chemistry and Physics*, 15, 2031–2049. <https://doi.org/10.5194/acp-15-2031-2015>

Publisher's Note Springer Nature remains neutral with regard to jurisdictional claims in published maps and institutional affiliations.

Springer Nature or its licensor (e.g. a society or other partner) holds exclusive rights to this article under a publishing agreement with the author(s) or other rightsholder(s); author self-archiving of the accepted manuscript version of this article is solely governed by the terms of such publishing agreement and applicable law.